ESA CONTRACT REPORT

Contract Report to the European Space Agency

Validation of aerosol parametrization - Representing aerosol processes in NWP

November 2009

Authors: J.-J. Morcrette and L. Jones

WP-2200 report for ESA contract 1-5576/07/NL/CB:
Project QuARL - Quantitative Assessment of the Operational Value of Space-Borne Radar and Lidar Measurements of Cloud and Aerosol Profiles

European Centre for Medium-Range Weather Forecasts
Europäisches Zentrum für mittelfristige Wettervorhersage
Centre européen pour les prévisions météorologiques à moyen terme

ECMWF

Series: ECMWF - ESA Contract Report

A full list of ECMWF Publications can be found on our web site under:
http://www.ecmwf.int/publications/

Contact: library@ecmwf.int

European Centre for Medium-Range Weather Forecasts
Shinfield Park, Reading, RG2 9AX, England

Contract Report to the European Space Agency

Validation of aerosol parametrization - Representing aerosol processes in NWP

Authors: J.-J. Morcrette and L. Jones

WP-2200 report for ESA contract 1-5576/07/NL/CB:
Project QuARL - Quantitative Assessment of the Operational Value of Space-Borne Radar and Lidar Measurements of Cloud and Aerosol Profiles

European Centre for Medium-Range Weather Forecasts
Shinfield Park, Reading, Berkshire, UK

November 2009

ABSTRACT

This report first presents a short history of prognostic aerosols in large-scale models of the atmosphere. It then quickly surveys the main parametrisations required for representing the physical processes affecting the aerosols. References are also given of the formulations used in the Integrated Forecasting System (IFS) of the European Centre for Medium-range Weather Forecasts (ECMWF).

As an illustration of the possibilities of the forecast system used in the GEMS-AERosol project (Global and regional Earth-system Monitoring using Satellite and in-situ data), one day worth of simulated aerosols is compared with cloud and aerosol quantities derived from the observations on-board the A-train constellation of satellites in order to validate the vertical distribution of the model aerosols. A good agreement is found over most areas in terms of the horizontal distribution of the model aerosols. Whereas the vertical distribution of model aerosols appears generally reasonable, the available CALIPSO-derived cloud/aerosol mask does not allow to validate the presence of aerosols in clouds in areas of deep convection, which seems prevalent in the model.

Contents

1 Introduction **1**

2 Aerosol processes to be accounted for **2**

2.1 Emission 2

2.2 Removal processes 3

3 Aerosols in the GEMS project **3**

4 Description of aerosol model parametrization in the ECMWF IFS **4**

5 The observational data **5**

6 Results **5**

6.1 Dust aerosols 7

6.2 Sea salt aerosols 7

6.3 Anthropogenic aerosols 7

6.4 Cloud-aerosol overlap 7

7 Conclusion and perspectives **32**

A List of Acronyms **34**

1 Introduction

There is a long history of regional and general circulation models, usually developed for climate studies, including a prognostic representation of aerosols. While developing the first regional model including such aerosols, Giorgi (1986b) pioneered efficient parametrisations for dry and wet deposition (Giorgi, 1986a; Giorgi and Chameides, 1986) from process studies linked to laboratory measurements or in-situ observations (Slinn and Slinn, 1980; Slinn, 1982; Monahan *et al.*, 1986). In the following years, a number of climate-oriented groups developed global models including a prognostic aerosol with a focus on one or another aerosol type (e.g., dust for Joussaume (1990); Tegen and Fung (1994); carbonaceous aerosols for Liousse *et al.* (1996); sea salt for Genthon (1992); Gong *et al.* (1997); sulfate for Chin *et al.* (1996)). In parallel to these efforts, models were also tested for their conservation properties (Guelle *et al.*, 1998; Dentener *et al.*, 1999). Looking at another methodological aspect, experiments were also run aiming at defining the best configuration to ensure reasonable aerosol forecasts (Jeuken *et al.*, 1996; Feichter and Lohmann, 1999). By the mid-90's, the aerosol modelling community felt that a climate GCM run at relatively low resolution from "cold-start" or climatological initial conditions would likely be diverging in terms of its main prognostic variables (temperature, pressure, wind, humidity) and thus would make the associated aerosol variables unrealistic. Most aerosol simulations (apart from climate simulations following climate scenarios such as those run for the Intergovernmental Panel on Climate Change model intercomparison) use atmospheric forcings (in terms of pressure, temperature, humidity, wind, ...) derived from meteorological analyses or re-analyses (see AEROCOM web site). This has the advantage that the meteorology follows the real day-to-day synoptic variability and verification can focus on the aerosol model.

The first multi-aerosol model simulations, often run with a forcing of the basic meteorology from an operational analysis every six, 12 or 24 hours, started to appear at the end of the 1990s (Tegen *et al.*, 1997) and have been the common set-up ever since (Guelle *et al.*, 2000; Clarke *et al.*, 2001; Chin *et al.*, 2002; Grini *et al.*, 2002; Penner *et al.*, 2002; Gong *et al.*, 2003; Liu *et al.*, 2003; Shao *et al.*, 2003; Zhao *et al.*, 2003; Reddy *et al.*, 2004). The first simulations assimilating some aerosol information were done for INDOEX by Collins *et al.* (2001) and Rasch *et al.* (2001) with the help of a chemical-transport model. In most of this second-generation prognostic aerosol models, most aerosol types were accounted for (sea salt, dust, organic and black carbon, sulphates). The package of aerosol physical parametrisations included the representation of the sources (interactive with the host model for the sea salt and dust aerosols), and of the gravitational sedimentation, dry deposition and wet deposition by precipitation together with the hygroscopicity effects on carbonaceous aerosols. The sulphur cycle was introduced (Boucher *et al.*, 2002; Chin *et al.*, 2002) with a simplified representation of the chemistry linking the chemical precursors to the sulphate aerosols.

Since then, a number of GCMs have been carrying out prognostic aerosols, usually to study the sensitivity of the climate to aerosols. A survey of those, as of 2008, with details on the prognostic representation of the aerosols, details on the parametrisations in use, and comparisons of the optical properties, and radiative forcing linked to the aerosols can be found in Kinne *et al.* (2003, 2006), Schulz *et al.* (2006), and Textor *et al.* (2006, 2007). Regional models have also been upgraded to represent (some) aerosol processes. For example, as part of the World Meteorological Organization Sand and Dust Storm Warning and Assessment System (WMO/SDS-WAS http://www.wmo.int/sds-was), eight models (six of them regional ones) are now run pre-operationally to simulate the dust burden of the atmosphere over the European region and a number of models will soon provide similar dust forecasts over the Asian region.

Despite the large number of models including prognostic aerosols, relatively few actually include an analysis of aerosol-related observations for operational or pre-operational weather forecasts. Such an analysis is used to define the best aerosol initial conditions to start a subsequent weather forecast including aerosol-related parameters. For example, the Chinese Meteorological Service (Zhou *et al.*, 2008) assimilates either satellite-retrieved index of column amounts of dust aerosol or surface visibility as observed by the meteorological sta-

tions of the Chinese Meteorological Administration for their regional model. The US Naval Research Laboratory has started a full operational system mid-October 2009 (http://www.nrlmry.navy.mil/aerosol/), which includes MODIS observations of the aerosol optical depth at 550 nm (τ_{550} over the ocean in its analysis (Zhang *et al.*, 2005, 2008; Zhang and Reid, 2006). The Goddard Global Modeling and Assimilation Office (GMAO) uses the Goddard Chemistry Aerosol Radiation and Transport (GOCART; Chin *et al.*, 2002) with MODIS τ_{550} to provide an analysis of aerosol optical depth and speciation (http://gmao.gsfc.nasa.gov/research/aerosol/), whereas ECMWF with some pre-operational analysis and forecast (http://gems.ecmwf.int/d/products/aer/realtime/) started in July 2008 producing such near-real time analysis and forecast. Similar effort has also been reported including the assimilation of CALIPSO observations via a 4-dimensional Ensemble Kalman Filter approach by Sekiyama *et al.* (2009) for the National Institute of Environmental Studies of Japan.

In this report the work related to the validation of aerosol parametrizations is presented in the following way: the aerosol emission and removal processes are addressed in Section 2, the GEMS-Aerosol project is briefly discussed in Section 3. Section 4 describes briefly the state of the ECMWF forecast model including aerosol processes. Section 5 introduces the CALIPSO/CloudSat observational data used to validate/verify the (horizontal and) vertical distribution of the aerosol plumes produced by the model. As an illustration of the possibilities (and deficiencies) of the model, in Section 6, the vertical distribution of the model aerosols (which up to the launch of CALIPSO had been impossible to assess on a global scale) is compared over one day-worth of A-train observations. Conclusions and perspectives for the potential use of EarthCARE aerosol-related observations to help with the aerosol modelling are presented in Section 7.

2 Aerosol processes to be accounted for

2.1 Emission

For the natural aerosols (sea salt SS, dust DU, dimethyl sulphide DMS), the emission is usually directly linked to the state of the model surface via parametrisations.

A review of the processes involving marine aerosols (whether sea salt or DMS based) can be found in O'Dowd *et al.* (1997) Different approaches to sea salt production are reviewed by Guelle *et al.* (2001) and a detailed description of the processes involved is given by Grini *et al.* (2002). They include the generation of sea spray by wind stress on the ocean surface, either from air bubbles in the whitecaps, or at higher wind speeds, from spume drops torn directly from the wave crests (Smith *et al.*, 1993). A parametrisation of the emission of sea salt aerosols has been proposed by Monahan *et al.* (1986), then revised by Smith and Harrison (1998) for the droplets between 2 and 4 μm. Similar source functions have been proposed by Vignati *et al.* (2004), Grini *et al.* (2002), Schulz *et al.* (2004), and Witek *et al.* (2007a,b). Corresponding DMS production is given in Boucher *et al.* (2002).

Dust mobilization is sensitive to a wide range of factors including soil composition, soil moisture, surface conditions, and wind velocity close to the surface. Various parametrisations have been developed over the years to represent the dust uplift to the atmosphere (Gillette *et al.*, 1980; Marticorena and Bergametti, 1995; Tegen and Fung, 1994; Ginoux *et al.*, 2001; Laurent *et al.*, 2008; Uno *et al.*, 2006; Zhao *et al.*, 2006). Morcrette *et al.* (2008) recently looked at how gustiness could be included in the 10-m wind used for diagnosing the emission of dust (and sea salt).

Sources for the other aerosol types are usually taken from inventories or databases. In the past, GFED (Global Fire Emission Database), SPEW (Speciated Particulate Emission Wizard), EDGAR (Emission Database for Global Atmospheric Research) were providing annual mean or monthly mean climatologies, until more recently more temporally resolved data (eight day inventories) have started to become available

(GFED-8d). Overall, these datasets include sources of organic and black carbon, and sulphate aerosols linked to fire emissions, both natural and anthropogenic, plus emissions from domestic, industrial, power generation, transport and shipping activities. More details on the sources of aerosols are given in Dentener *et al.* (2006).

2.2 Removal processes

Several types of removal processes have to be considered: i/ the dry deposition including the turbulent transfer to the surface, ii/ the gravitational settling, iii/ the wet deposition including rainout (by large-scale and convective precipitation within the clouds) and washout of aerosol particles below the clouds. Hygroscopic effects have also to be accounted for.

A review of the knowledge on dry deposition, taking into account the surface type (ocean or land, vegetation type) is given in Wisely and Hicks (2000). Gravitational settling of aerosols is accounted for following Massey (1987) or similar to settling of ice particles in cirrus (Tompkins, 2005). GCM-type schemes to deal with wet precipitation scavenging have been given by Lee and Feichter (1995) and Rasch *et al.* (2000). New developments in in-cloud and below-cloud scavenging in the ECHAM-HAM climate model are described in Croft *et al.* (2009a,b).

3 Aerosols in the GEMS project

As part of the project Global and regional Earth-system Monitoring using Satellite and in-situ data (GEMS, Hollingsworth *et al.*, 2008), the European Centre for Medium-range Weather Forecasts (ECMWF) is developing its assimilation system to include observations pertaining to greenhouse gases, reactive gases and aerosols. For the computation of the trajectory forecast used in the assimilation, the Integrated Forecast System (IFS) has been extended to include a number of tracers, which are advected by the model dynamics and interact with the various physical processes.

With respect to the aerosols, sources have thus been added to the model, and a representation of the aerosol physical processes (namely the interactions of the aerosols with the vertical diffusion and the convection, plus the sedimentation, dry deposition and wet deposition by large-scale and convective precipitation) are now part of the package of physical parametrisations of the ECMWF IFS model.

ECMWF/GEMS also uses the strategy outlined in the Introduction by running the atmospheric model plus aerosol module in a 12-hour cycle where the atmospheric initial condition is taken from the operational analysis and the aerosols from the previous 12-hour forecast. This guarantees that the atmospheric flow remains close to the analyses and has the advantage that meteorology and aerosol modelling are fully integrated.

Given the final requirement of having not only the direct version of the aerosol routines, but also the tangent-linear and adjoint versions of the same aerosol routines of the model for use in the four-dimensional variational assimilation, a certain level of simplification has to be considered when accepting an existing parametrisation from the literature or designing a new one for the model. In this respect, the emphasis is somewhat different from that of the representation of aerosols in a general circulation model used for climate studies where aerosol processes may have a sophisticated representation in order to be able to handle various sensitivity studies. Here, the forecast model including aerosols will be used at relatively high resolution, both horizontally and vertically, to provide information on the aerosol loading over the time-scale of a few hours to a few days. In consequence, the dynamical transport is of primary importance in such forecasts. It is therefore important to simulate the aerosol loading (and in the future, aerosol radiative forcing and possible impact of aerosols on clouds) on a monthly mean time scale, but it is even more important

that the correct monthly means are obtained from an accurate representation of the short-term variability of the aerosol distributions. During its development phase, much effort has been spent on validating the overall horizontal distribution of the model aerosols through comparisons with MODIS (MODerate resolution Imaging Spectroradiometer: Remer *et al.*, 2005) and MISR (Multi-angle Imaging SpectroRadiometer) satellite-derived aerosol optical depth (Morcrette *et al.*, 2009; Benedetti *et al.*, 2009). Also the temporal variability of the aerosol loading was validated through extensive comparison with aerosol optical depth (http://gems.ecmwf.int) observed at various wavelengths by AERONET (AErosol ROboticNETwork: Holben *et al.*, 1998; Dubovik *et al.*, 2002; Kinne *et al.*, 2003).

4 Description of aerosol model parametrization in the ECMWF IFS

A detailed description of the ECMWF forecast model including aerosol processes is given in Morcrette *et al.* (2008).

The initial package of ECMWF physical parametrisations dedicated to aerosol processes mainly follows the aerosol treatment in the LOA/LMD-Z model (Boucher *et al.*, 2002; Reddy *et al.*, 2005). Five types of tropospheric aerosols are considered: sea salt, dust, organic and black carbon, and sulphate aerosols. A prognostic representation of the stratospheric aerosols is not included here, as the period 2003-2004 considered for the initial model development was almost devoid of any sizeable amount of stratospheric aerosols (at least, from a radiative point of view). Similarly, the emission of aerosols by volcanoes is not present in the following results. Both types of aerosols will be considered in a later stage of the introduction of aerosols in the ECMWF IFS.

For all tropospheric aerosols, sources are defined, the sedimentation of all particles, and the wet and dry deposition processes are represented. For organic matter and black carbon, two components, hygrophobic and hygrophilic, are considered, and the transfer from hygrophobic to hygrophilic is also included. The sulphur cycle is considered via a precursor variable SO_2 transformed in a sulphate aerosol (SO_4) with a time-scale simply dependent on latitude (as in Huneeus and Boucher, 2007).

A bin representation is used in this study to include prognostic aerosols of natural origin (taken to mean sea-salt SS and dust DU). The maximum flexibility regarding the limits of the bins for the sea-salt and dust aerosols is allowed in the model. In the following, the sea-salt aerosols are tentatively represented by 3 bins, with limits at 0.03, 0.5, 5 and 20 microns. Similarly, the desert dust aerosols are represented by 3 bins with limits at 0.03, 0.55, 0.9, and 20 microns. The above limits are chosen so that roughly 10, 20 and 70 percent of the total mass of each aerosol type are in the various bins.

The two natural aerosols (SS and DU) have their sources only linked to some prognostic and diagnostic model variables. In contrast, the anthropogenic aerosols (organic matter OM, black carbon BC and SO_4) have their sources read from external data-sets. Sources of sea-salt and desert dust are interactive with surface and near-surface variables of the model. Sources for the other aerosol types are taken from the GFED, SPEW), and EDGAR annual- or monthly-mean climatologies until more temporally-resolved data are provided as part of the GEMS project. Overall, these datasets include sources of organic and black carbon, and sulphate aerosols linked to fire emissions, both natural and anthropogenic, plus emissions from domestic, industrial, power generation, transport and shipping activities.

Several types of removal processes are considered, the dry deposition including the turbulent transfer to the surface and the gravitational settling, and the wet deposition including rainout (by large-scale and convective precipitation) and washout of aerosol particles in and below the clouds. The wet and dry deposition schemes are standard, whereas the sedimentation of aerosols follows closely what was introduced by Tompkins (2005) for the sedimentation of ice particles. Hygroscopic effects are also considered for organic matter

and black carbon aerosols.

5 The observational data

Various sources of observational data have been used to verify the model aerosols (Morcrette *et al.*, 2009; Benedetti *et al.*, 2009). Recently the GEMS aerosols were used to assess the GlobAEROSOL database over the year 2004 (Peubey *et al.*, 2009). All such validations and assessments were limited to either that of the geographical/horizontal distribution of the aerosol plumes via comparison of the model aerosol optical depth τ_M with satellite-derived (MODIS, MISR, SEVIRI, MERIS, AATSR) τ_S or that of the temporal variability of τ_M via comparison of time-series of the aerosol optical depth observed at several wavelengths by AERONET.

Here, the CALIPSO lidar on the Aqua satellite provides vertical profiles of the aerosol extinction coefficient along the satellite track over a narrow track whereas the radar on-board CloudSat provides a similar information on clouds (Stephens *et al.*, 2002). In the following, the vertical distribution of aerosols and clouds along the A-Train track within the ECMWF IFS is qualitatively compared to the cloud-aerosol mask derived from combined CloudSat-CALIPSO observations (Vaughan *et al.*, 2005).

6 Results

For the results presented below, there is **no** assimilation of any data related to aerosol into the IFS, i.e., the results of the comparisons will only show the quality (or otherwise) of the aerosol forecasts. The model, including the parametrisations for the physical aerosol processes discussed in section 4, was run from a given initial date (20070515) in a series of forecasts starting every 12 hours from the ECMWF operational analyses. The model aerosols are free-wheeling, i.e., starting from null concentrations of aerosols on the initial date. The various aerosols are let to spin up for about 8-12 days (the time their contents establish themselves) with aerosols produced from surface emission fluxes, and going through the physical processes (dry deposition, sedimentation, hygroscopicity, wet deposition by large-scale and convective precipitation). The aerosols at the end of a given 12-hour forecast are passed as initial conditions at the start of the next 12-hour forecast. This is in essence not very different from what is done within conventional transport models, except for the fact that the aerosol processes are consistent with the dynamics and all other physical parametrisations.

The aerosol forecast presented below is one in a series of experimental near-real time 72-hour forecasts at $T_L159L91$ started on 15 May 2007 00UTC and going on since.

In pre-processing the model data, 00UTC forecast data on the model levels are retrieved every three hours from T+0 to T+27. The data is then interpolated in both space and time to the A-train orbit. From a given forecast, first all the CloudSat granule files are found that contain any data in the specific 27 hour period. Then those files are read and the orbit scanned from point to point, looking for where it crosses IFS grid-box boundaries. If two neighbouring CloudSat points are found to exist in different IFS grid-boxes, then a linear interpolation is done between them to find the ”exact” orbital crossing point. Then a second round of linear interpolations is done between pairs of crossing points to obtain a set of points which lie on the orbit (to within the accuracy dictated by the linear method) and for which there is one point for every IFS grid-box that the orbit passes through. These are the latitude-longitude points to which the IFS data is bi-linearly interpolated, and thus the resolution of the (irregular) interpolated data is the same as the resolution of the initial data. The spatial interpolation is done first, and is done for two fields at every point - the two fields whose validity times straddle the CloudSat orbital time at that point. Then the two spatially interpolated values are linearly interpolated to the correct time. Note that CALIPSO trails CloudSat by a few seconds,

so in the following plots, the time axes of the CloudSat and IFS plots line up, whereas the CALIPSO data is plotted for a slightly shifted time period in order to show the same spatial section. The line showing the ground in the IFS plots is the surface pressure as obtained from the model surface pressure. The very good agreement between the shape of the surface pressure curves and the ground height as directly measured by the satellites was the best confirmation that the spatial interpolation is working properly. In the following, comparisons are presented for all orbits over one day (26 June 2007) chosen randomly.

Although in this stage of the development of the ECMWF IFS, the aerosols are not interactive with the radiation scheme, the optical thicknesses for all aerosols have been evaluated as diagnostic quantities that can be compared to measurements such as those taken by AERONET, or derived from satellite measurements like those of MODIS or MISR. Such comparisons with AERONET, MODIS and MISR were at the core of the validation effort at the time of the development of the aerosol model (Morcrette *et al.*, 2009; Benedetti *et al.*, 2009), and are not repeated here.

In this report, we concentrate on the aspect of the model aerosol distribution, which had received little attention till now, namely on using CALIPSO observations to check the vertical distribution of model aerosols.

Table 6.1 describes the main characteristics of the areas covered by the various orbits.

Figure No.	time-slot	Area	Orbit	Main feature
1	00:36:29-01:00:01	Africa	D	dust
2	02:13:28-02:47:39	S.Atl.-Sahara	D	dust
3	04:00:12-04:26:20	Atlantic	D	dust
4	05:32:43-06:00:11	South Amer.-N. Atl.	D	biomass burning?
5	06:22:06-06:55:16	Asia-S.Indian	A	sea salt
6	07:11:12-07:42:17	S.Pac.-N.Amer.	D	anthropogenic
7	08:06:09-08:34:41	Centr.Asia-S.Indian	A	anthropogenic
8	09:40:02-10:00:00	Indian	A	sea salt
9	10:28:48-10:56:34	Pac.-Canada	D	sea salt
10	11:18:34-11:51:51	Centr.Eur.-Africa	A	dust
11	12:06:08-12:40:39	Pacific	D	sea salt
12	13:00:21-13:30:48	W.Eur.-Sahara-S.Atl.	A	dust
13	14:00:32-14:20:39	S.Pacific	D	sea salt
14	14:37:41-15:00:00	Atlantic	A	dust
15	15:25:42-15:58:44	Australia-Pac.	D	sea salt
16	16:14:19-16:48:16	N.Atl.-Brazil-S.Atl.	A	sea salt?
17	17:02:48-17:38:07	Austr.-W.Pac.-Japan	D	sea salt?
18	17:59:58-18:27:12	N.Amer.-S.Amer.	A	anthropogenic
19	19:31:43-20:00:00	N.Amer.-East Pac.	A	anthropogenic
20	20:19:30-20:57:47	Asia-S.Indian	D	sea salt-anthrop.
21	21:12:11-21:47:11	Pacific	A	sea salt
22	22:00:13-22:34:38	Centr.Asia-S.Indian	D	anthropogenic
23	23:00:19-23:25:35	N. Pacific	A	sea salt
24	23:38:19-00:00:00	W.Asia-NW.Africa	D	dust

Table 6.1: A-Train satellite observations: Time-slots, covered areas, main aerosol features. Uncertainty on the dominant aerosol type is indicated by a question mark.

6.1 Dust aerosols

Dust aerosols are characterized by large loads usually filling the lowest 500 hPa layer of the atmosphere as can be seen in Figures 6.1, 6.2, 6.3, 6.10, 6.12 and 6.24. For all these areas, the presence of a large aerosol load is also seen in the model, showing the successful representation of the sources by the current parameterization based on 10-m wind and surface parameters (surface UV-visible albedo derived from MODIS, soil moisture). However, the model seems to be transporting some of these aerosols to higher levels (Fig. 6.1 around 6^oN, Fig.6.2 around 12.5^oN, Fig. 6.10 around 45^oN and 15^oN, Fig. 6.12 around 12^oN, Fig. 6.24 between 5^oN and 16^oN), a feature that is not shown in the CALIPSO aerosol mask.

6.2 Sea salt aerosols

The signature of sea salt aerosols is usually restricted to the planetary boundary layer (generally below 800 hPa) and these aerosols often appear mixed with low-level stratiform cloudiness (Fig. 6.5 between 10^oS and 35^oS, Fig. 6.8 between 8^oS and 40^oS, Fig. 6.9 between 10^oN and 18^oS, Fig. 6.11 between 25^oN and 45^oS, Fig. 6.13 between 8^oN and 26^oS, Fig. 6.20 between 10^oS and 35^oS, Fig. 6.21 between 5^oN and 25^oS, Fig. 6.23 between 22^oN and 25^oS. The model usually produces a similar presence of sea salt aerosols, restricted to the lower levels of the atmosphere. In the model, these layers often include low-level clouds (Figs. 6.3, 6.8, 6.9, 6.11, 6.13, 6.20, 6.21 and 6.22). Overall, the corresponding optical depth for the model sea salt aerosols might be on the low side with values generally below 0.01.

6.3 Anthropogenic aerosols

In the other areas, given the geography and the prevailing circulation, the aerosols are much more likely to be of anthropogenic origin. Unfortunately, the aerosol forecast, run in near-real time conditions at the time, was relying on monthly climatologies for black carbon, organic matter and sulphate emissions. Figure 6.4 shows a reasonable agreement between the observed and modelled vertical distributions of aerosols over South America and the northern Atlantic. However, for other areas (Figs. 6.6, 6.7, 6.17, 6.18, 6.19 and 6.20), the agreement is much poorer with the model displaying too large and too widely spread (both horizontally, along the satellite track, and vertically) compared to the observation-derived cloud/aerosol mask. One feature prevalent in the model is the strong vertical transport (likely by convection) of aerosols. This can be seen in the model panel in Fig. 6.6 around 35^oN, Fig. 6.7 around 30^oN, Fig. 6.17 between 30^oN and 50^oN, Fig.6.18 between 20 ^oN and 36^oN, Fig. 6.19 between 8^oN and 40^oN, Fig. 6.20 between 26^oN and 7^oS, Fig. 6.22 between 10^oN and 25^oN.

6.4 Cloud-aerosol overlap

The mask derived from CALIPSO observations classifies atmospheric features in terms of cloud, aerosol, stratospheric cloud, surface or attenuated (area under cloud where the signal is too much attenuated to give useful information). In that respect, it acts as an either/or filter and does not allow, for example, the presence of both cloud and aerosol in the same layer. Such a combination of cloud and aerosol is quite common in the model forecast, particularly in areas where convection is active (Figs. 6.1, 6.5, 6.7, 6.9, 6.10, 6.15 to 6.20, 6.22 to 6.24). At this stage, it is impossible to say whether the model actually displays too strong a transport by convection.

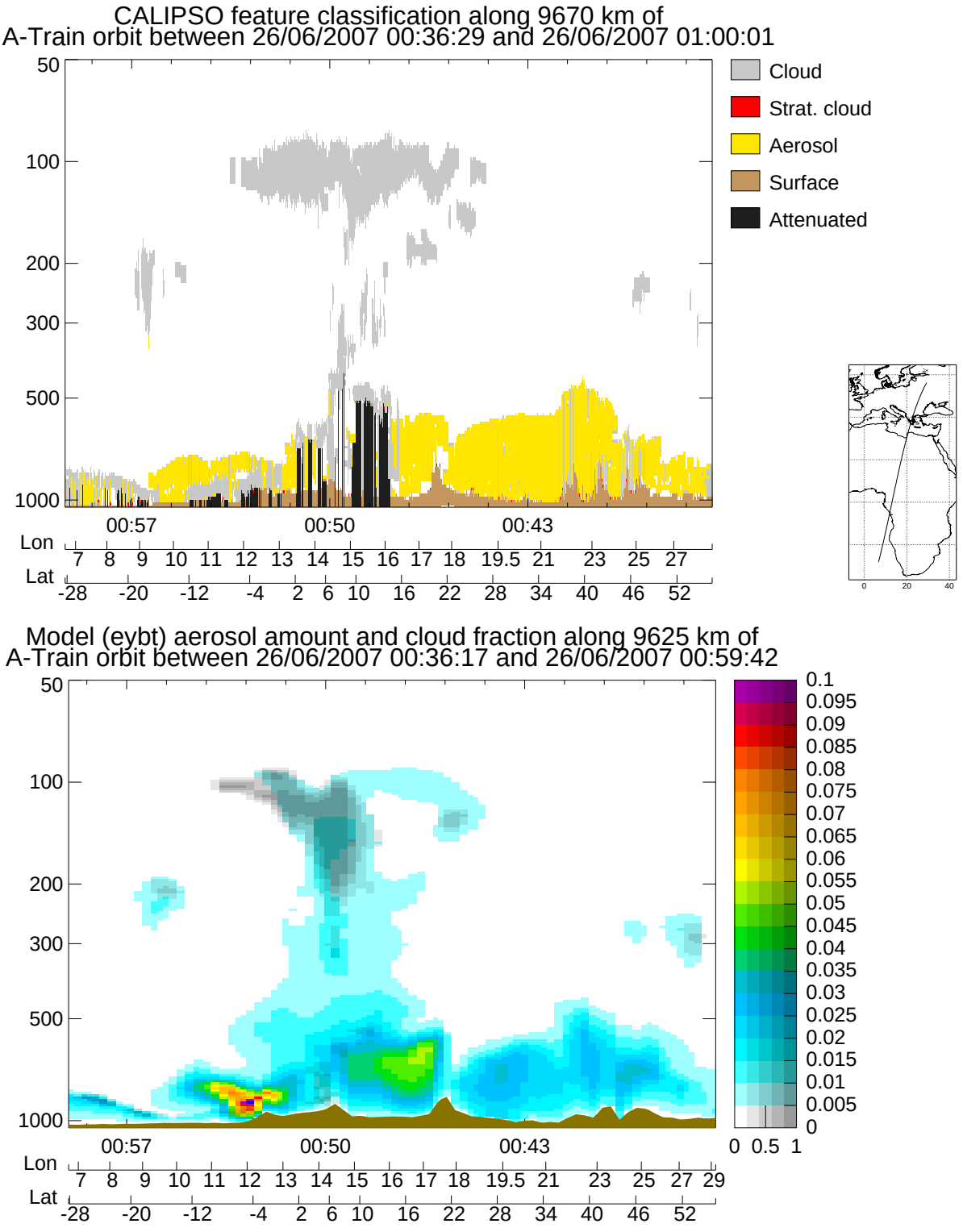

Figure 6.1: The CALIPSO classification on 20070626 for the A-train orbit between 00:36:29 and 01:00:01 (top panel). The corresponding cloud (horizontal grey scale) and aerosol (vertical colour scale) profiles from the IFS Model (bottom panel), and the corresponding orbit track (middle right panel).

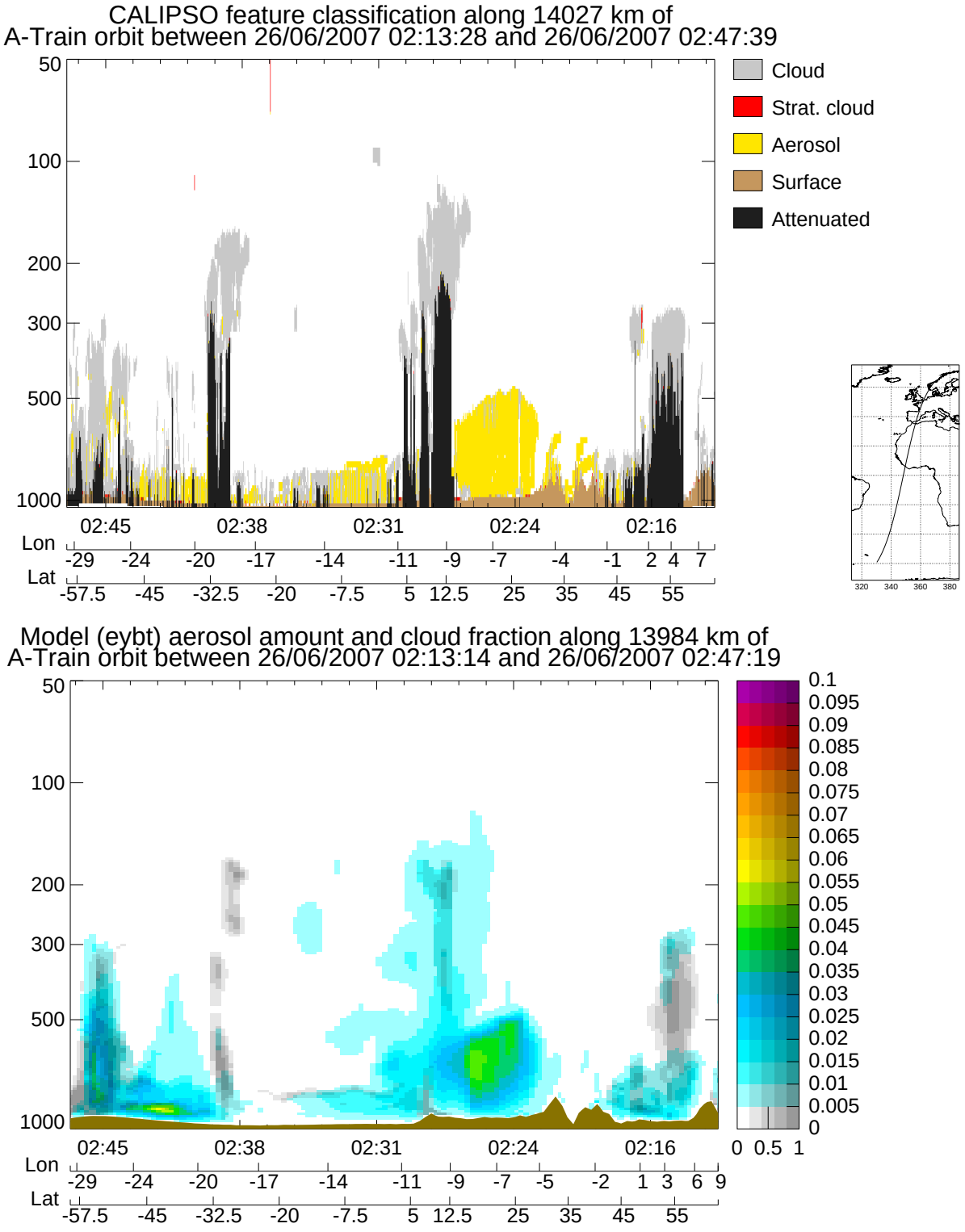

Figure 6.2: As in Figure 6.1, but for the orbit between 02:13:28 and 02:47:39.

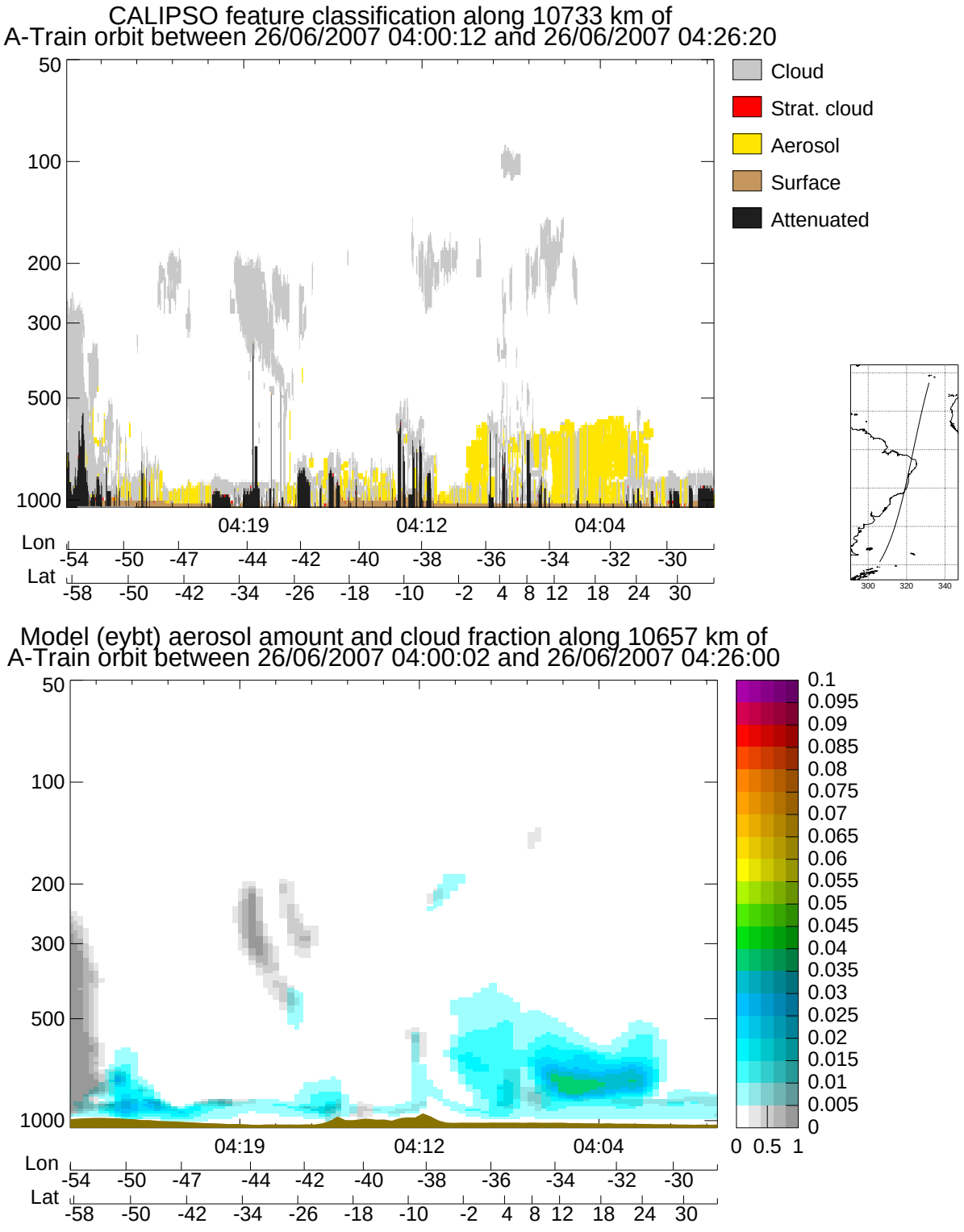

Figure 6.3: As in Figure 6.1, but for the orbit between 04:00:12 and 04:26:20.

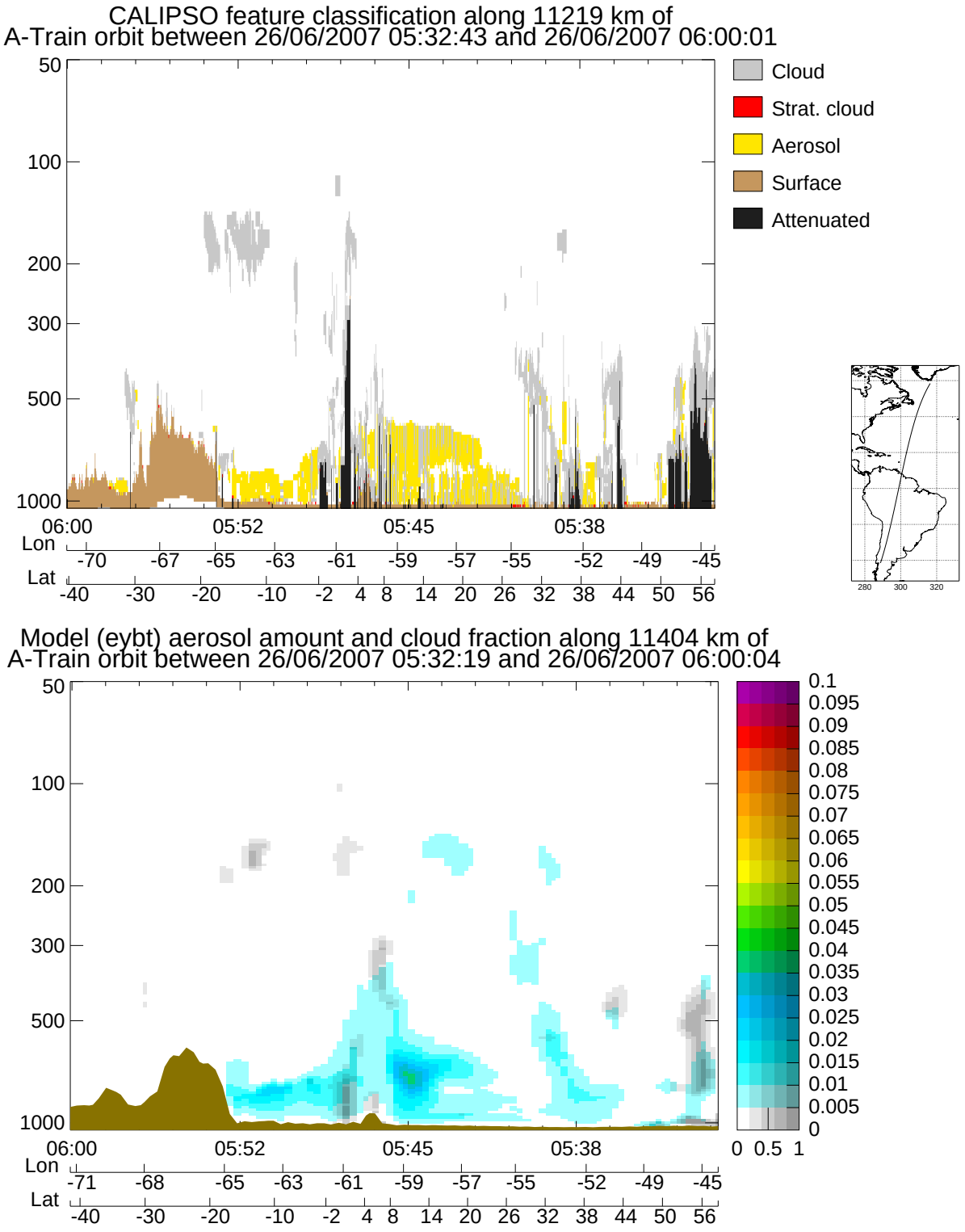

Figure 6.4: As in Figure 6.1, but for the orbit between 05:32:43 and 06:00:01.

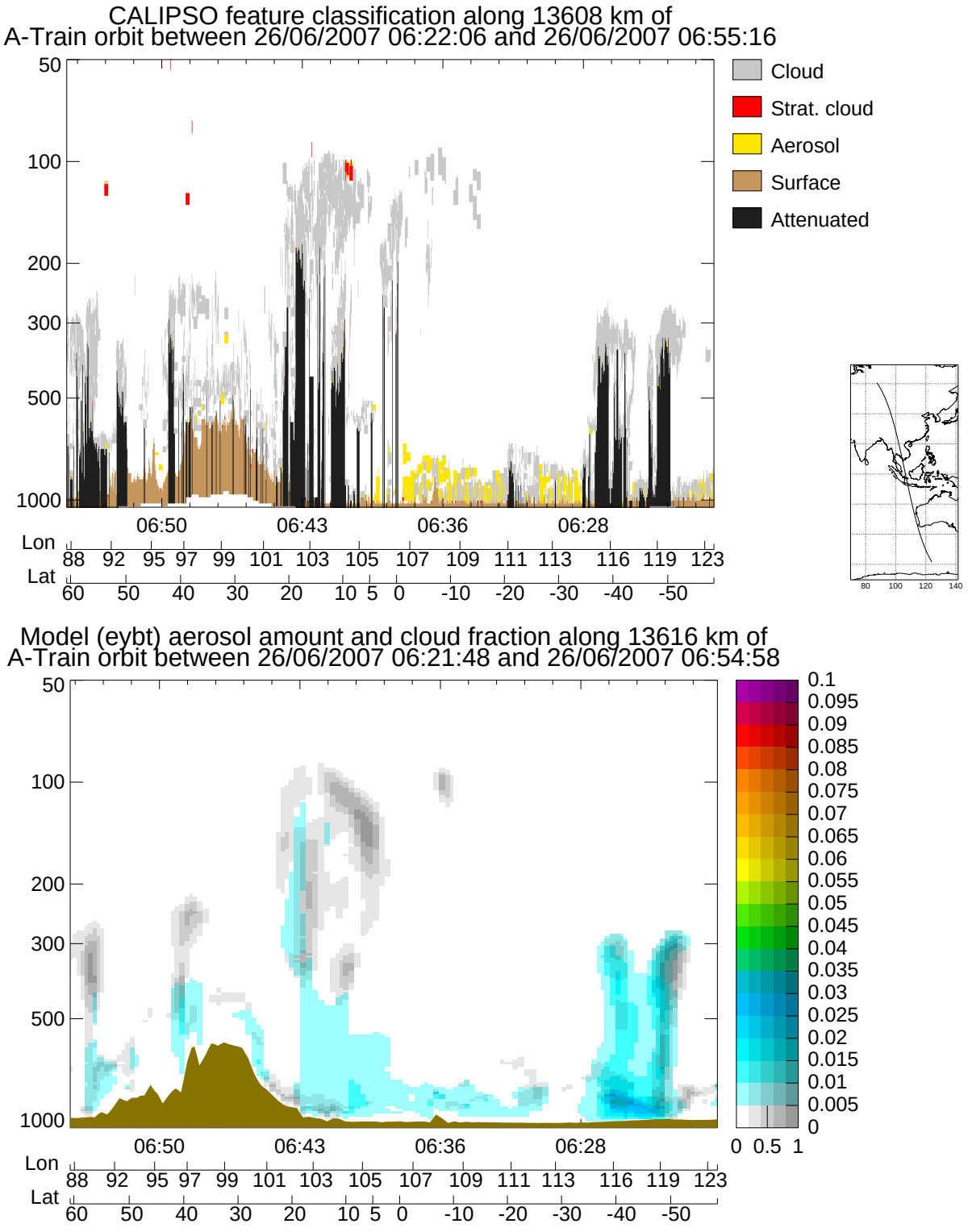

Figure 6.5: As in Figure 6.1, but for the orbit between 06:22:06 and 06:55:16.

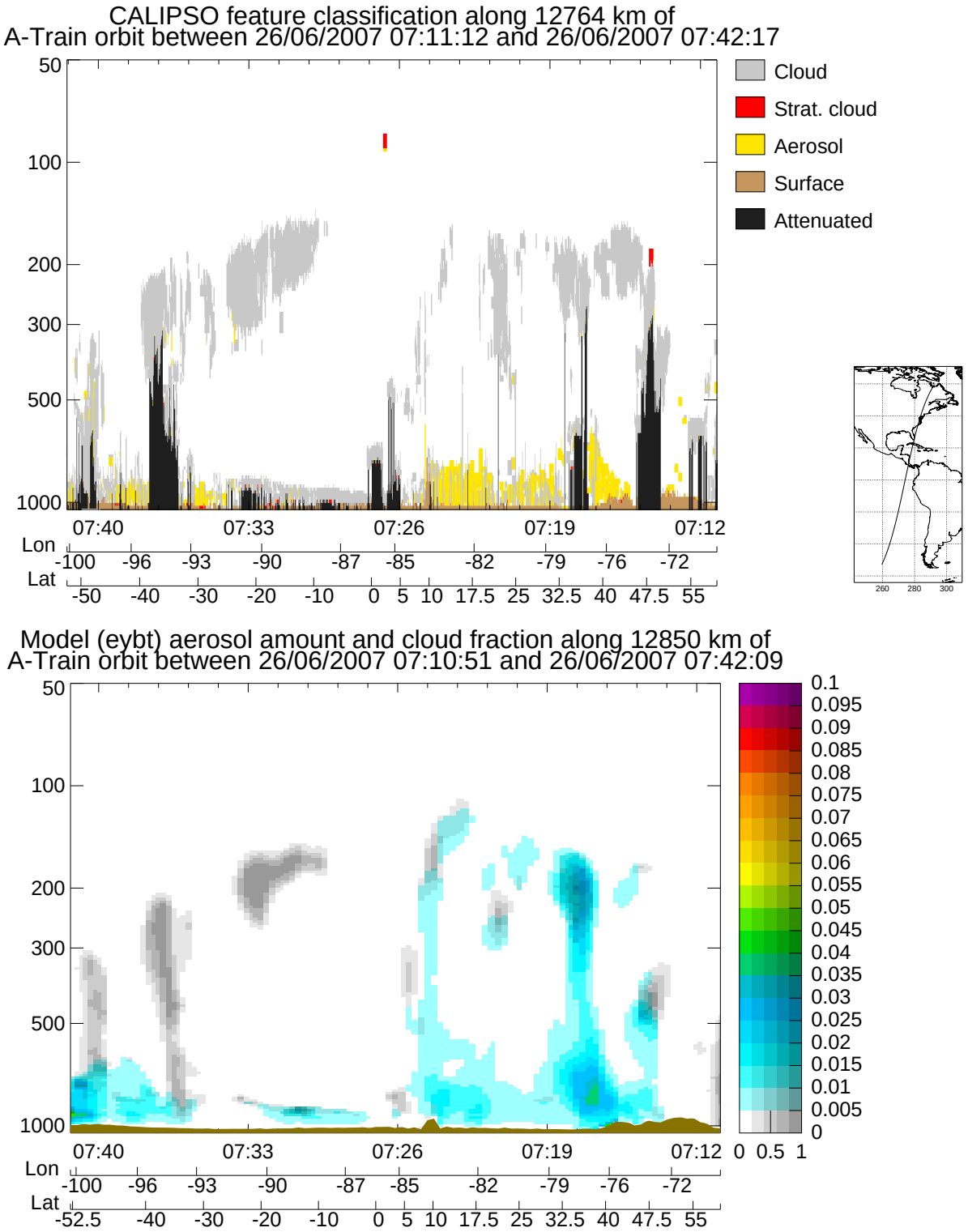

Figure 6.6: As in Figure 6.1, but for the orbit between 07:11:12 and 07:42:17.

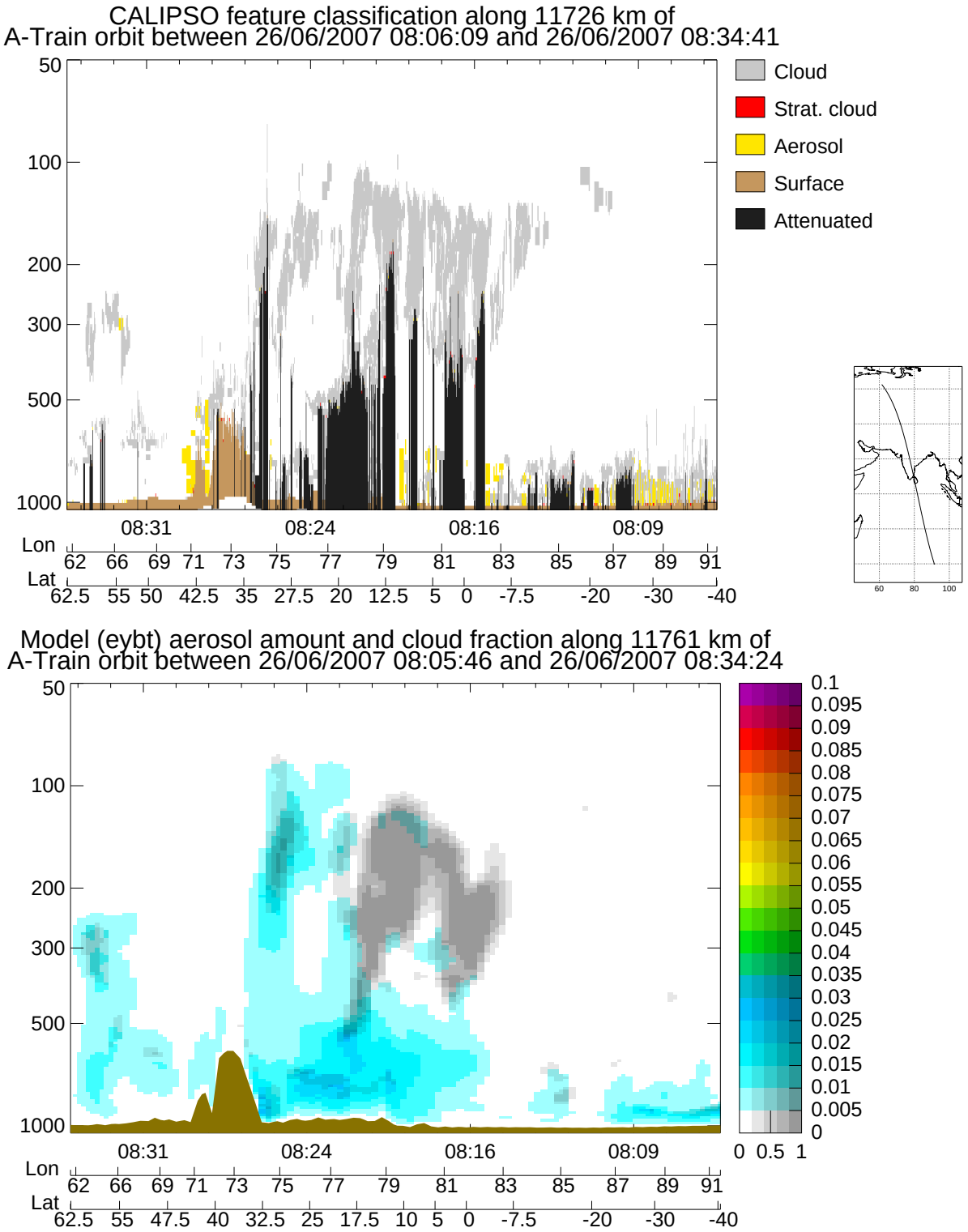

Figure 6.7: As in Figure 6.1, but for the orbit between 08:06:09 and 08:34:41.

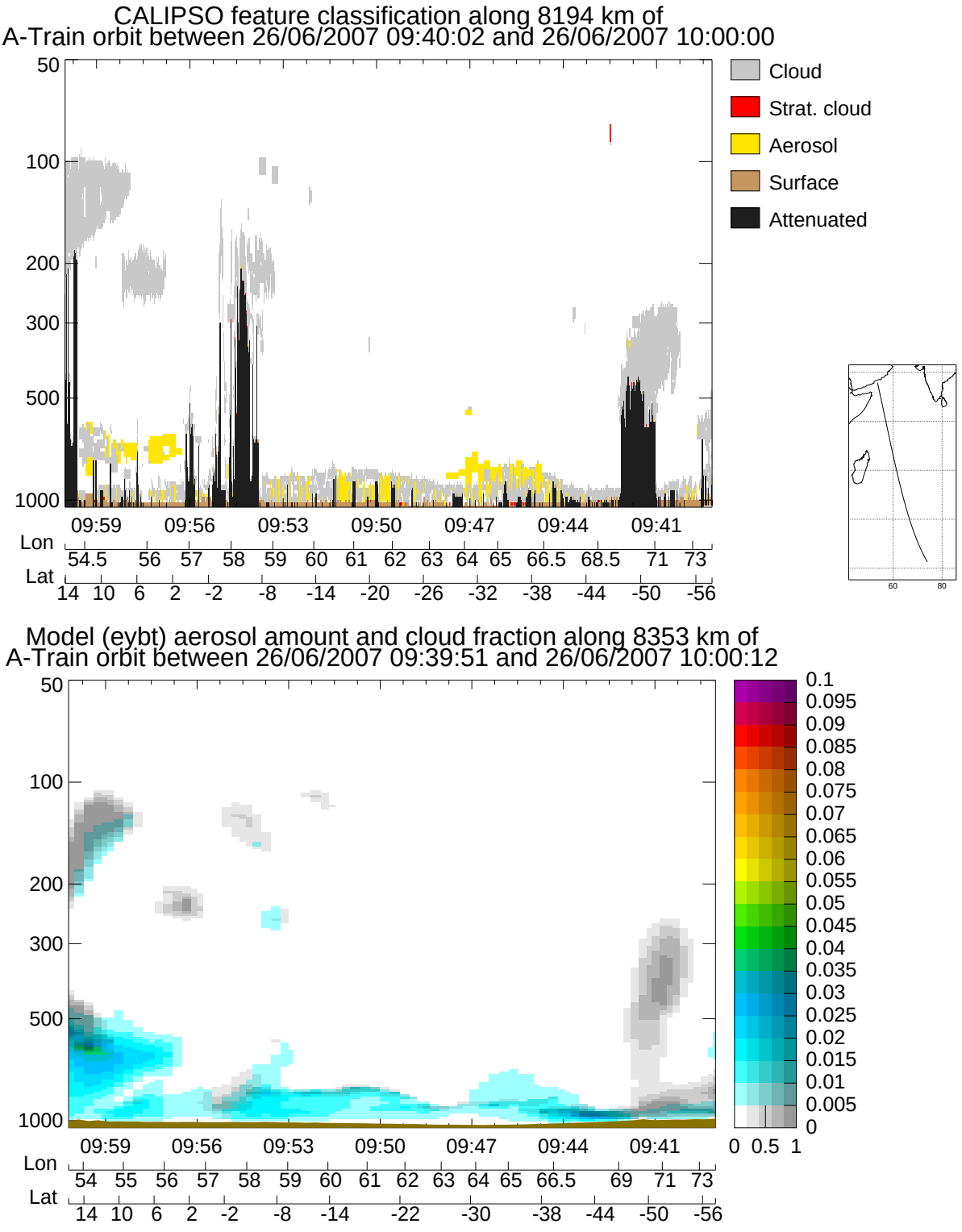

Figure 6.8: As in Figure 6.1, but for the orbit between 09:40:02 and 10:00:00.

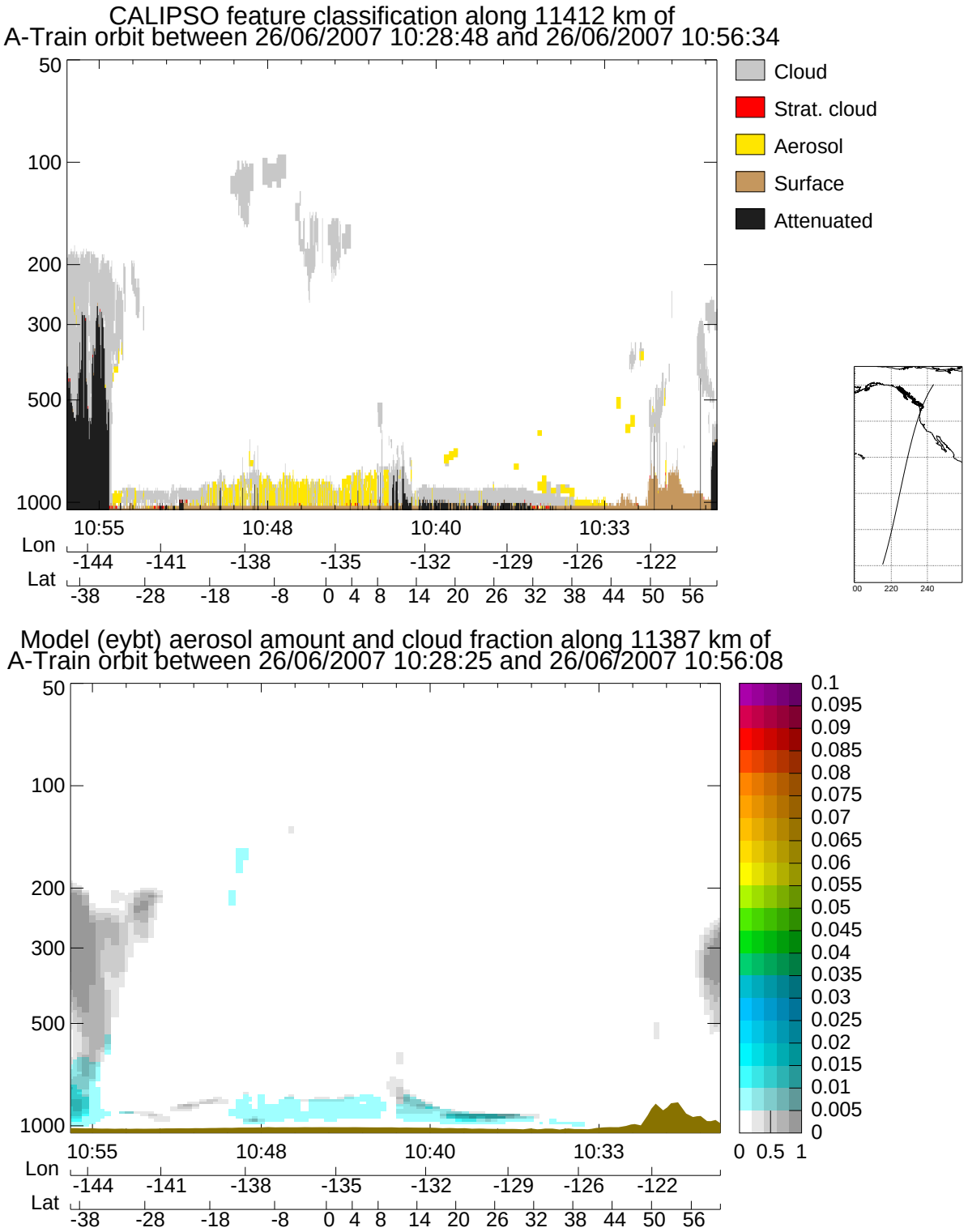

Figure 6.9: As in Figure 6.1, but for the orbit between 10:28:48 and 10:56:34.

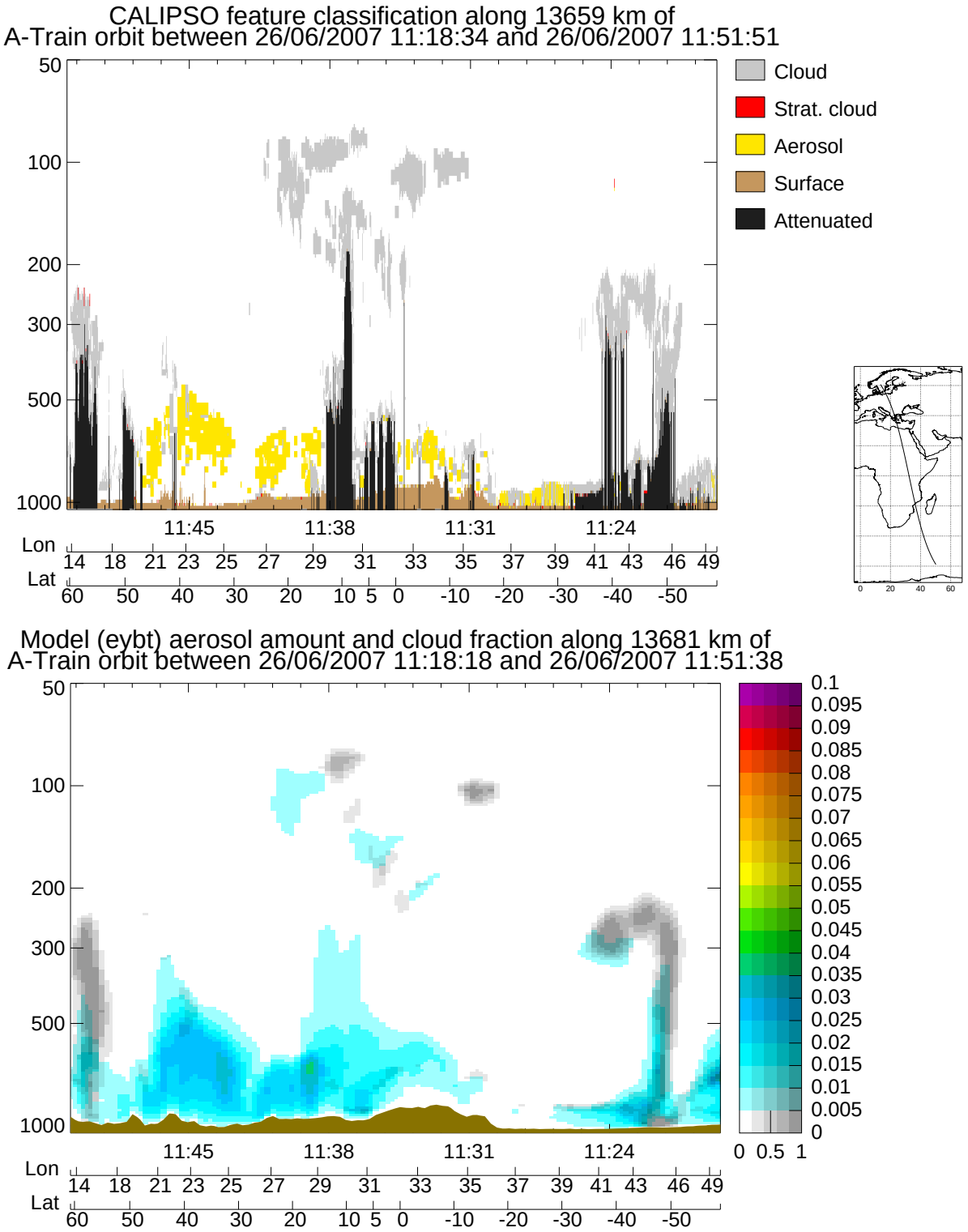

Figure 6.10: As in Figure 6.1, but for the orbit between 11:18:34 and 11:51:51.

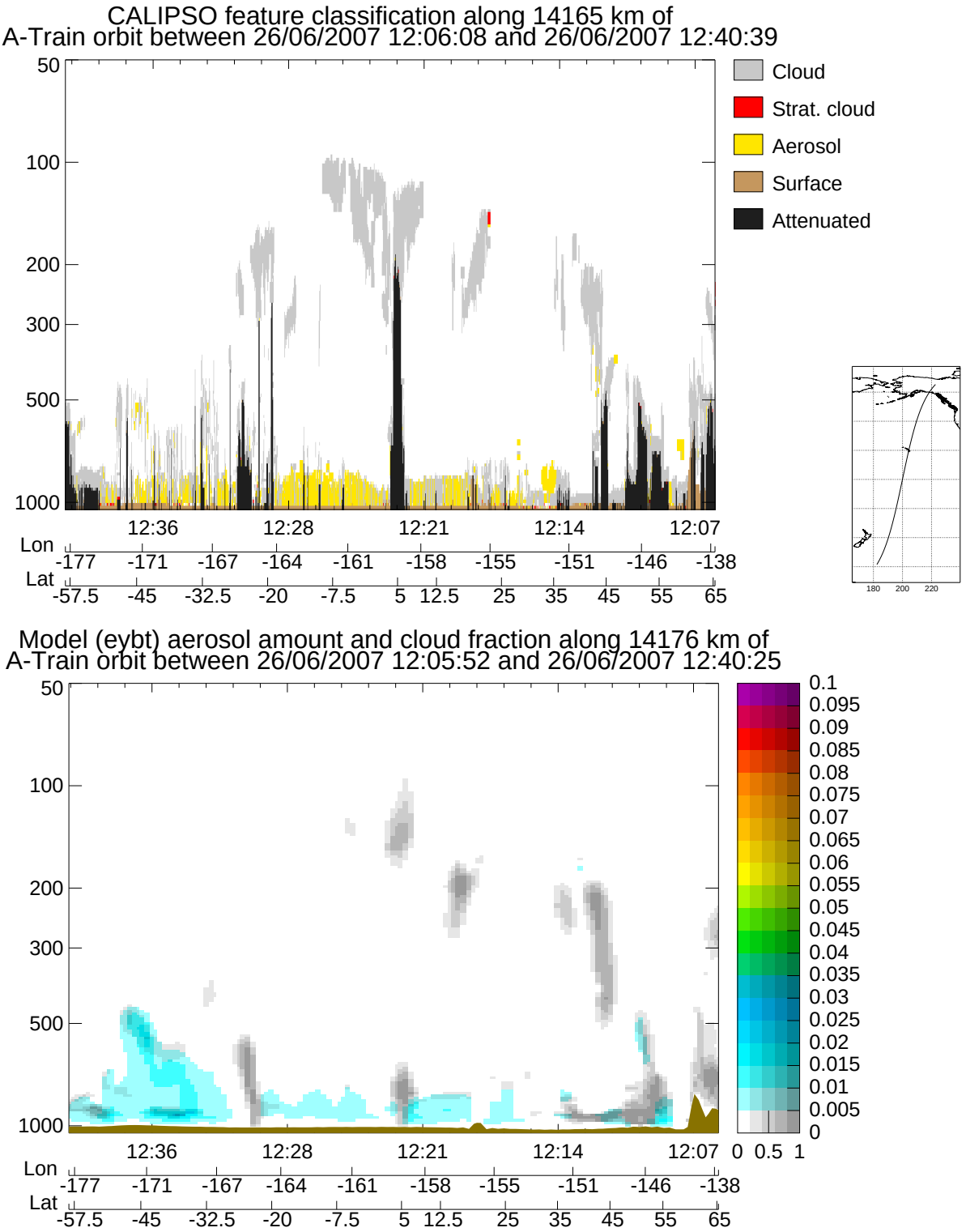

Figure 6.11: As in Figure 6.1, but for the orbit between 12:06:08 and 12:40:39.

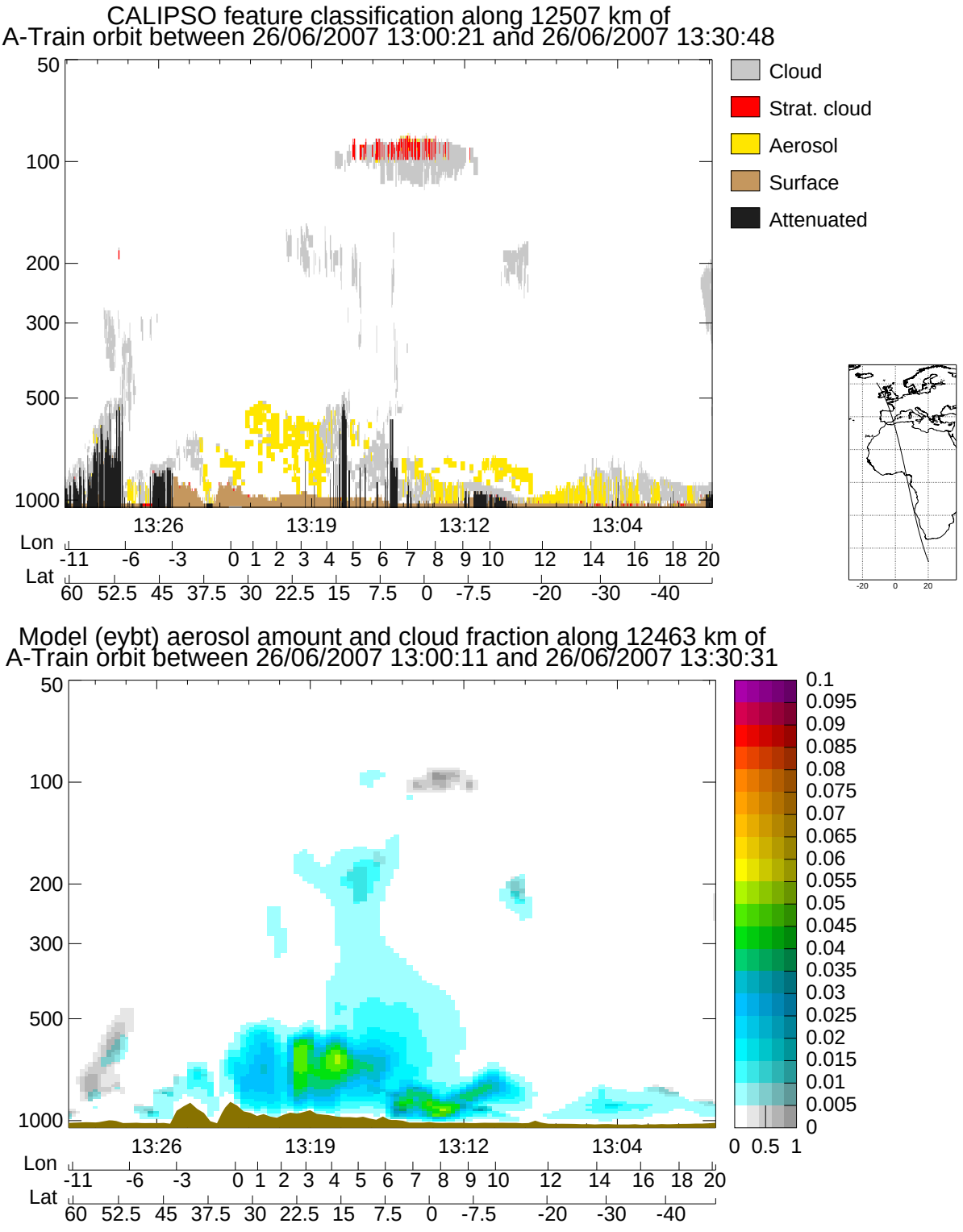

Figure 6.12: As in Figure 6.1, but for the orbit between 13:00:21 and 13:30:48.

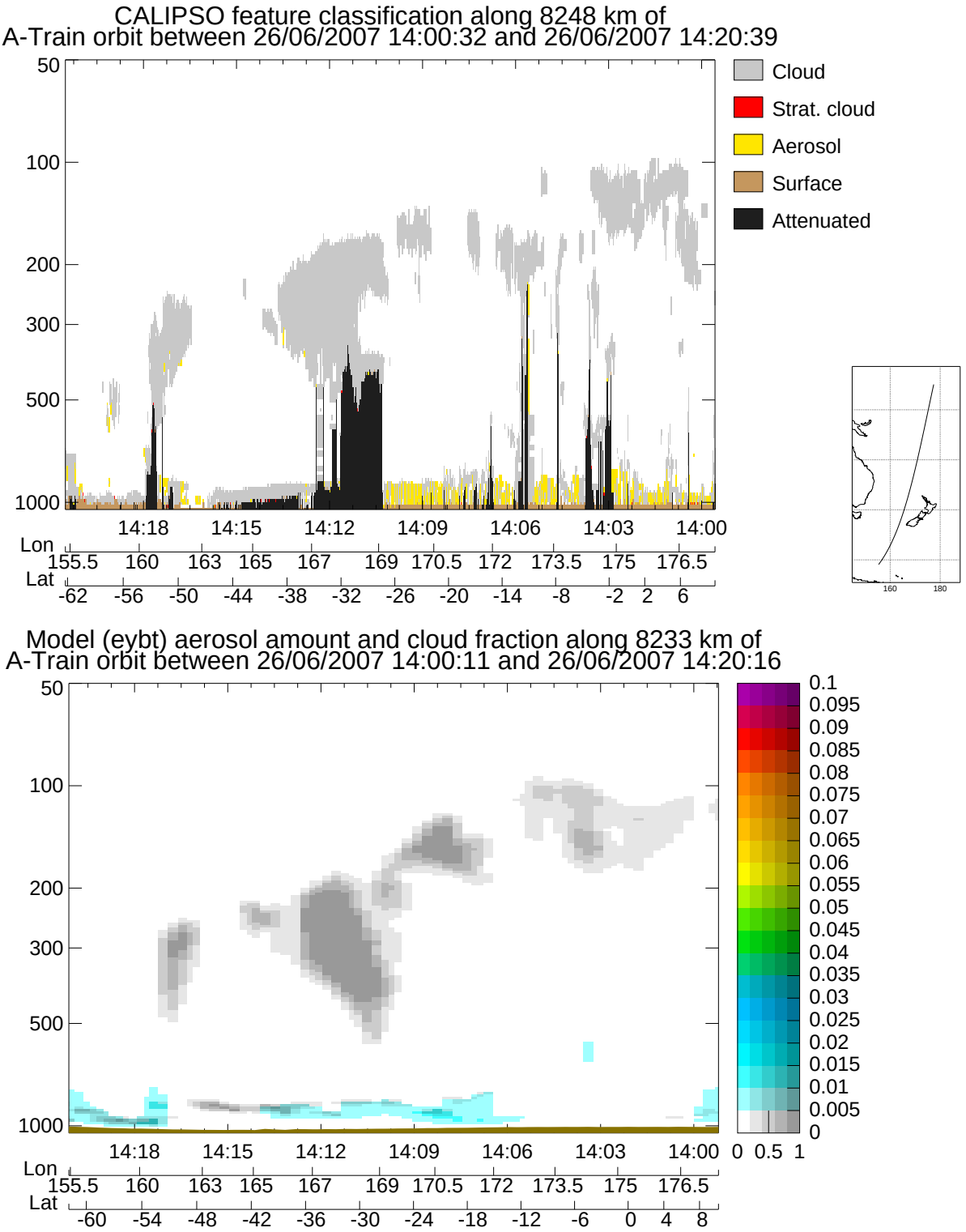

Figure 6.13: As in Figure 6.1, but for the orbit between 14:00:32 and 14:20:39.

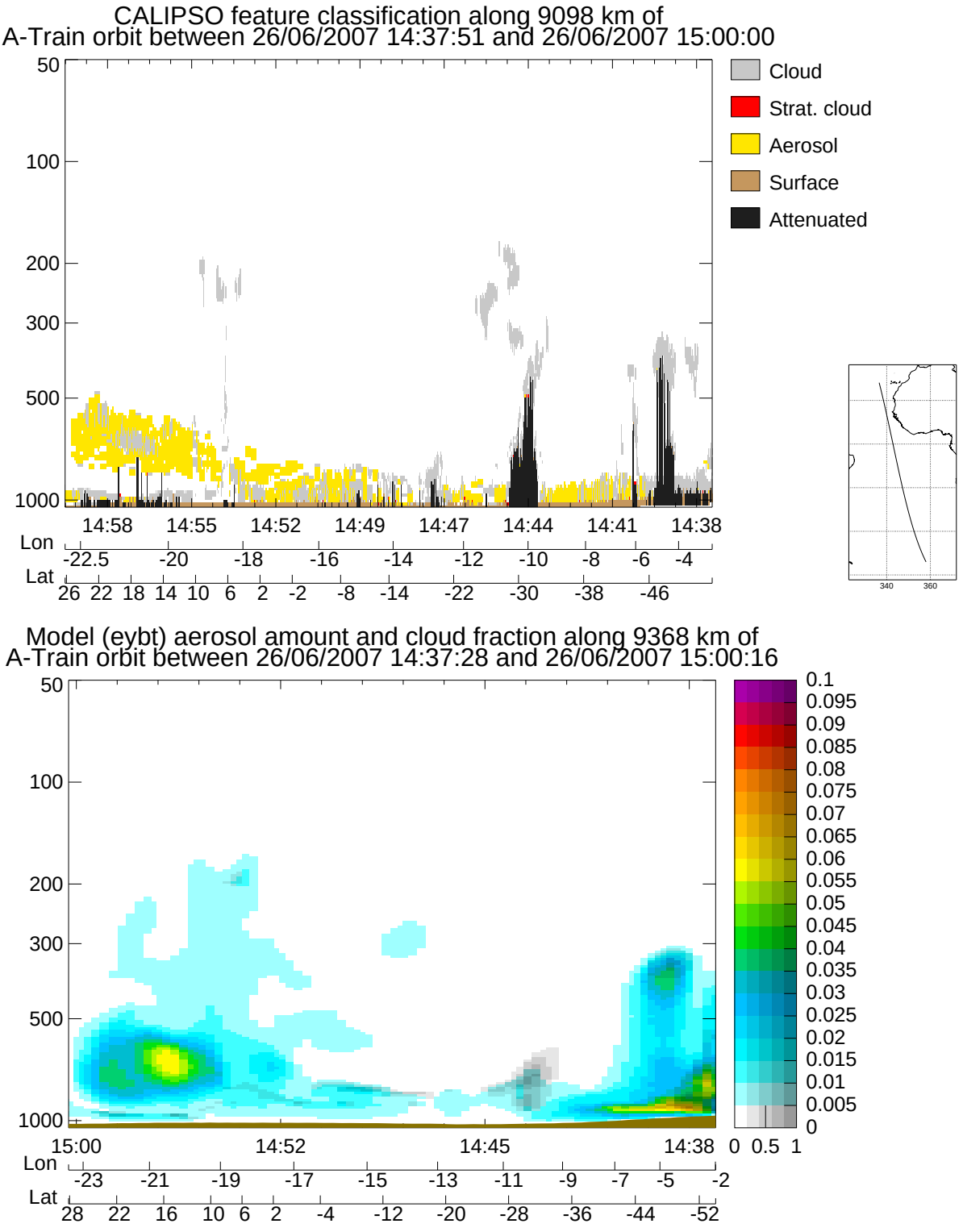

Figure 6.14: As in Figure 6.1, but for the orbit between 14:37:51 and 15:00:00.

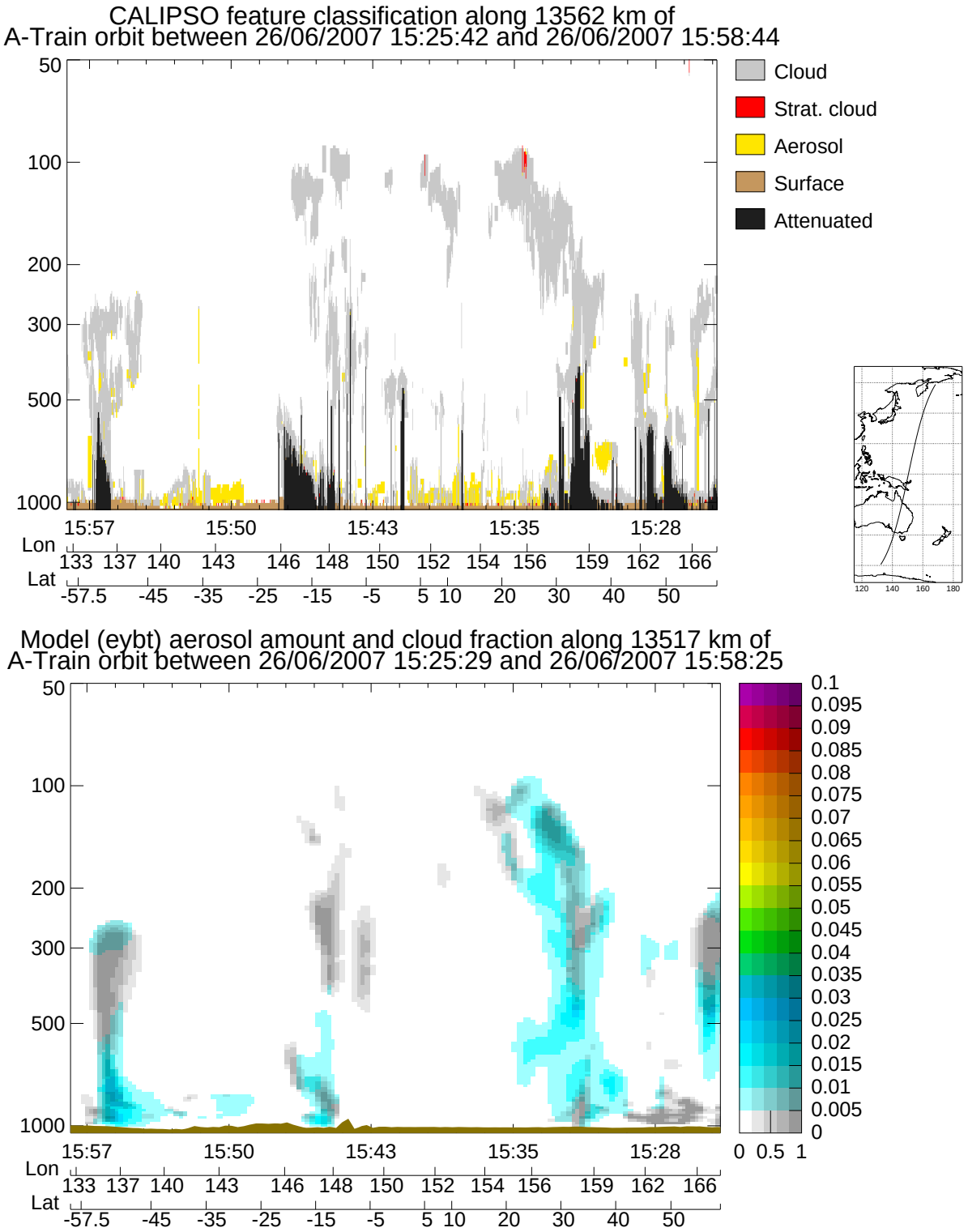

Figure 6.15: As in Figure 6.1, but for the orbit between 15:25:42 and 15:58:44.

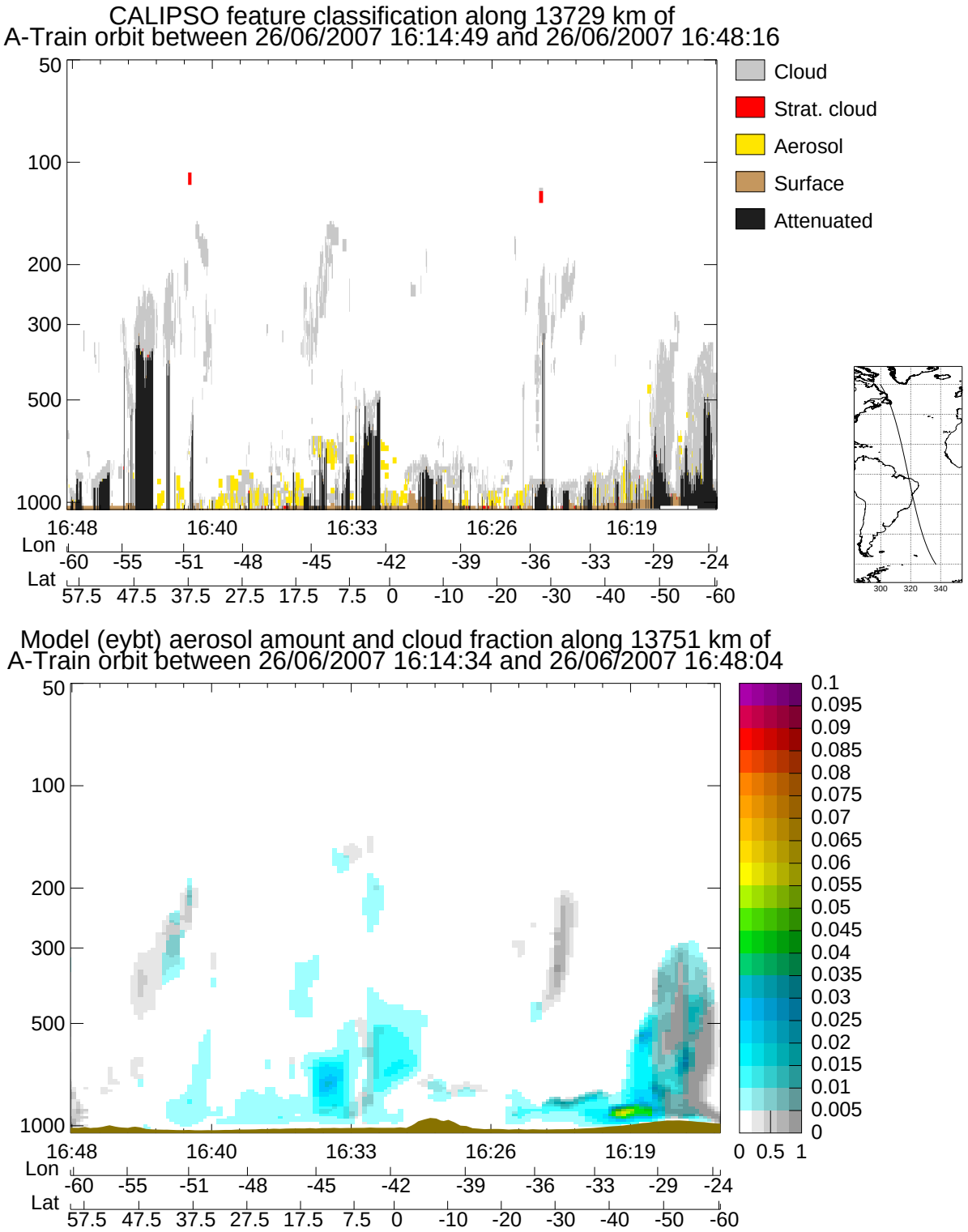

Figure 6.16: As in Figure 6.1, but for the orbit between 16:14:49 and 16:48:16.

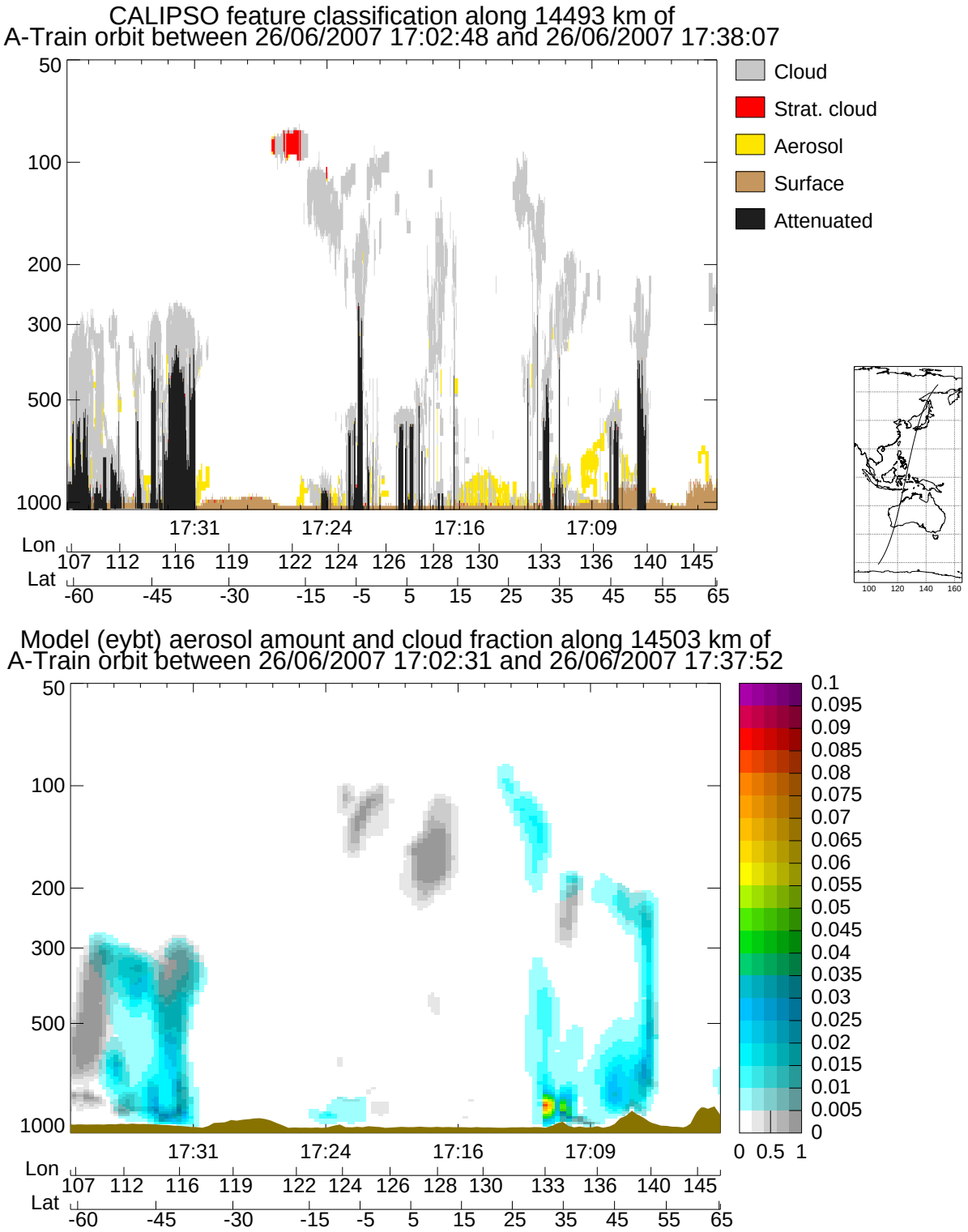

Figure 6.17: As in Figure 6.1, but for the orbit between 17:02:48 and 17:38:07.

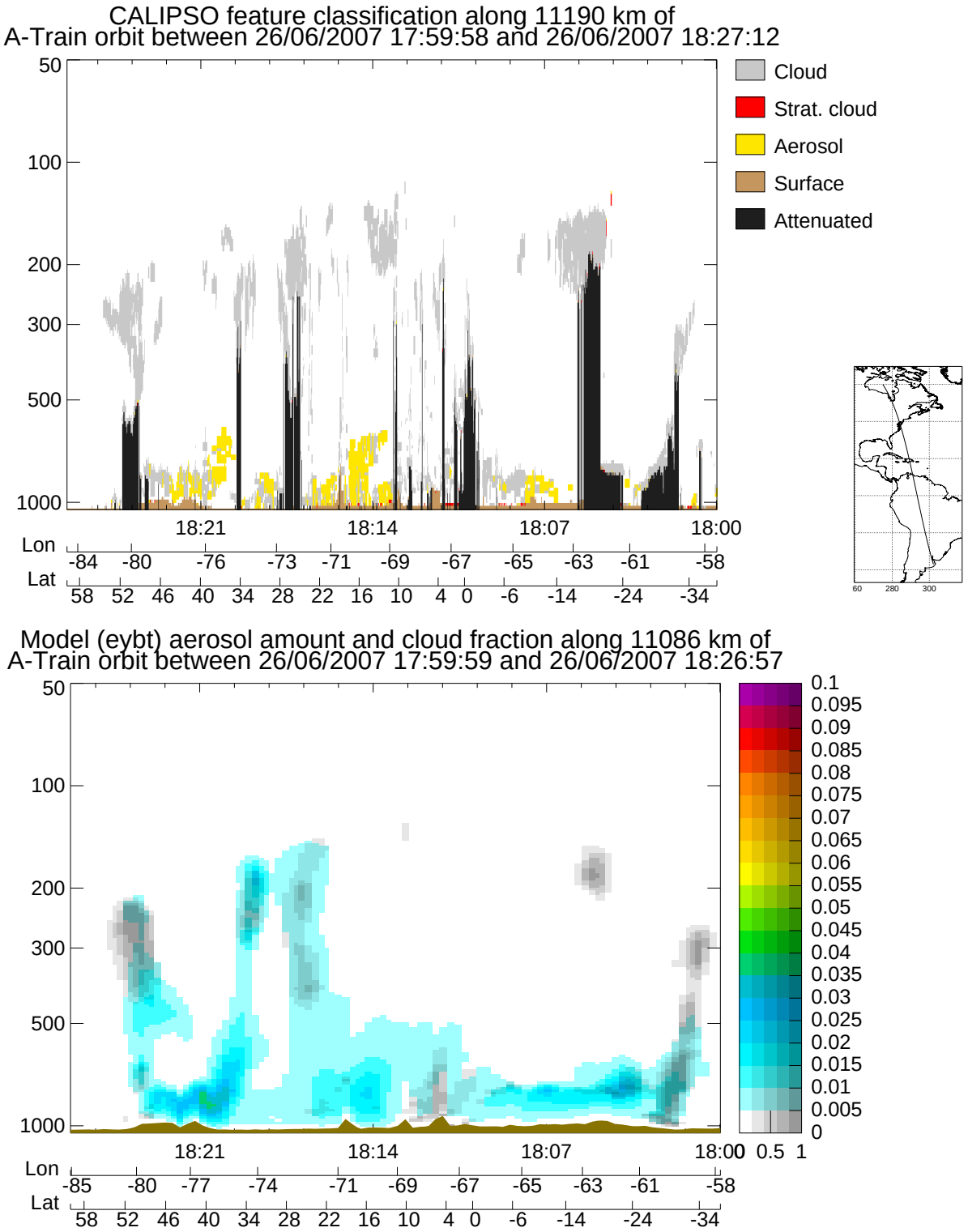

Figure 6.18: As in Figure 6.1, but for the orbit between 17:59:58 and 18:27:12.

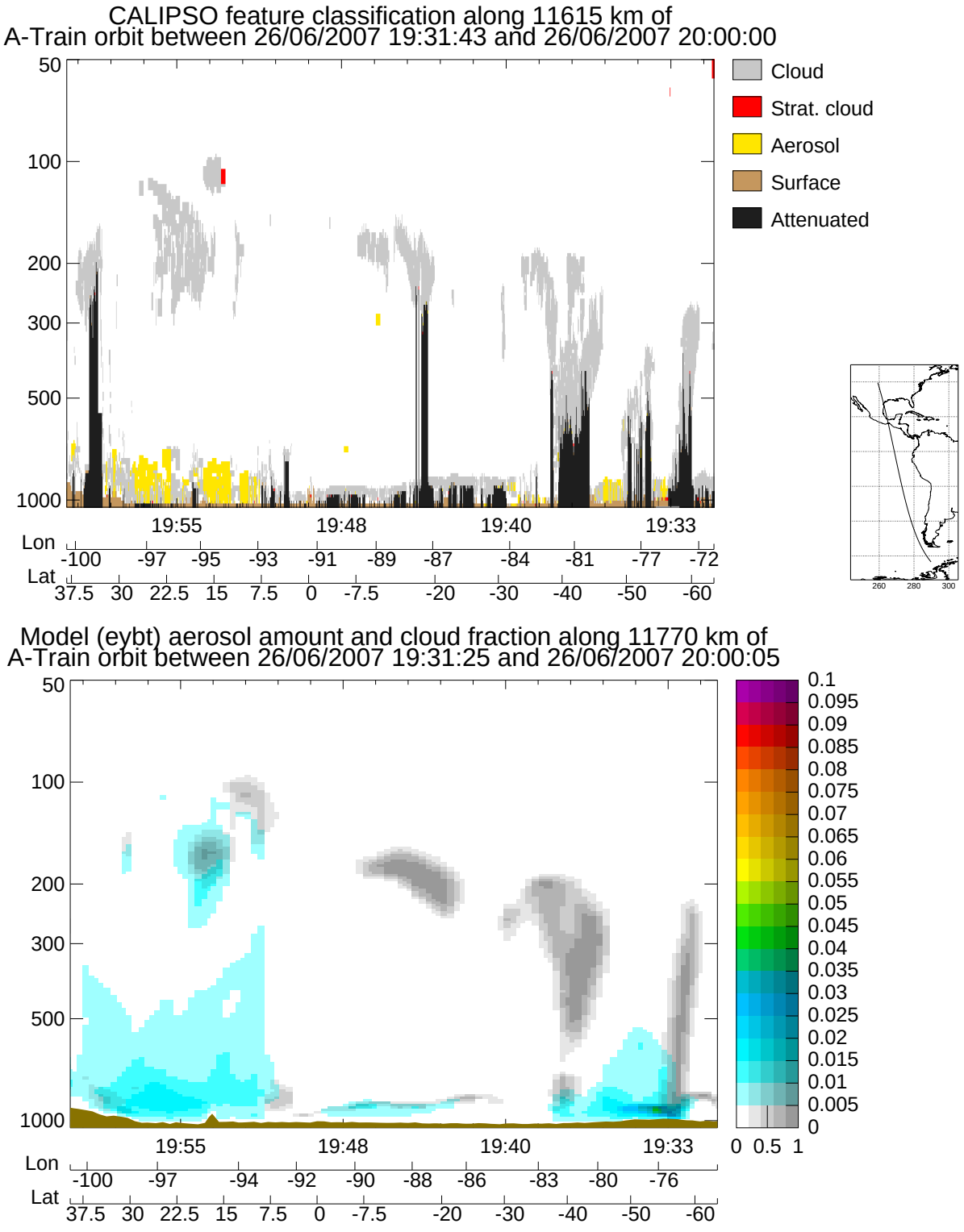

Figure 6.19: As in Figure 6.1, but for the orbit between 19:31:43 and 20:00:00.

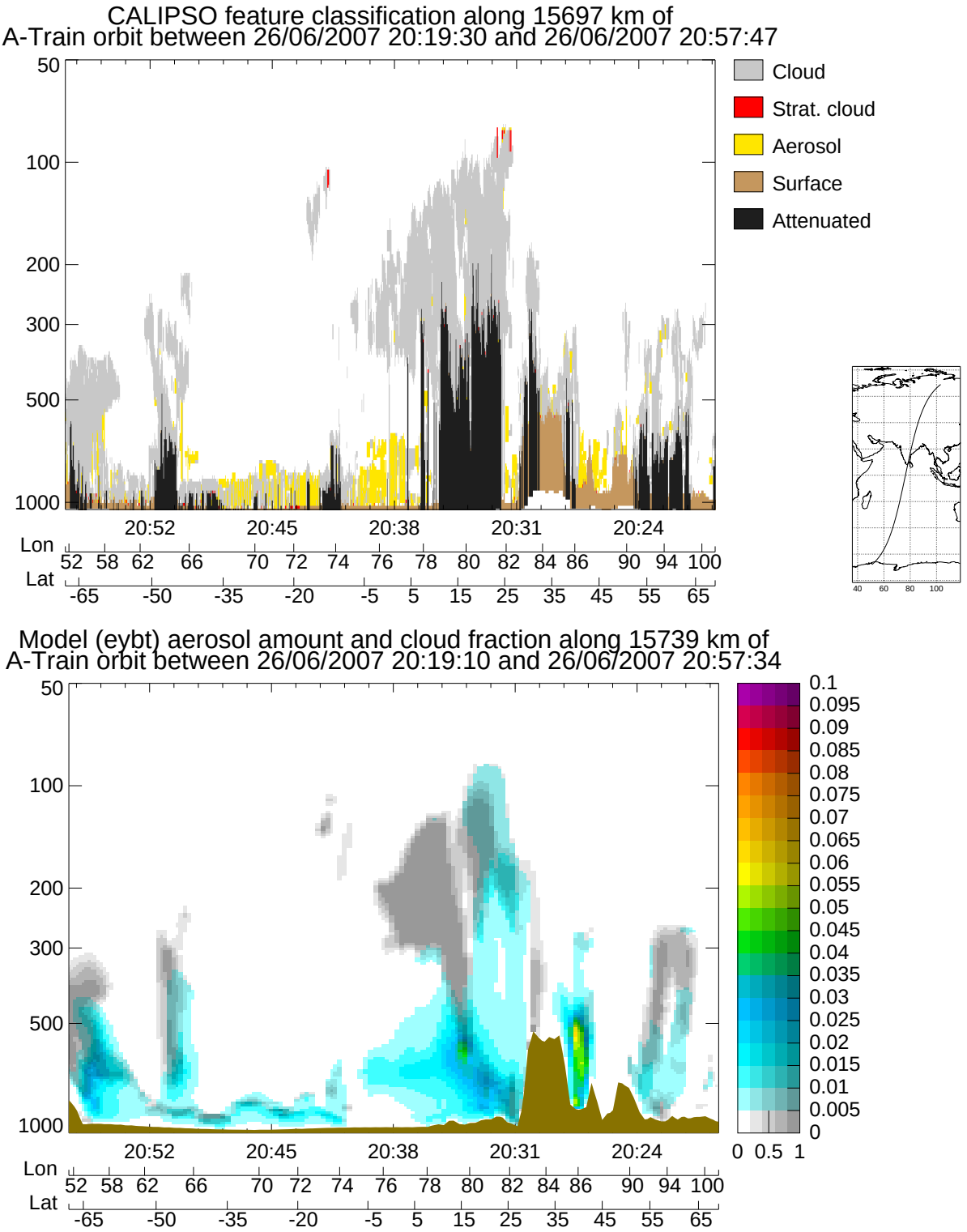

Figure 6.20: As in Figure 6.1, but for the orbit between 20:19:30 and 20:57:47.

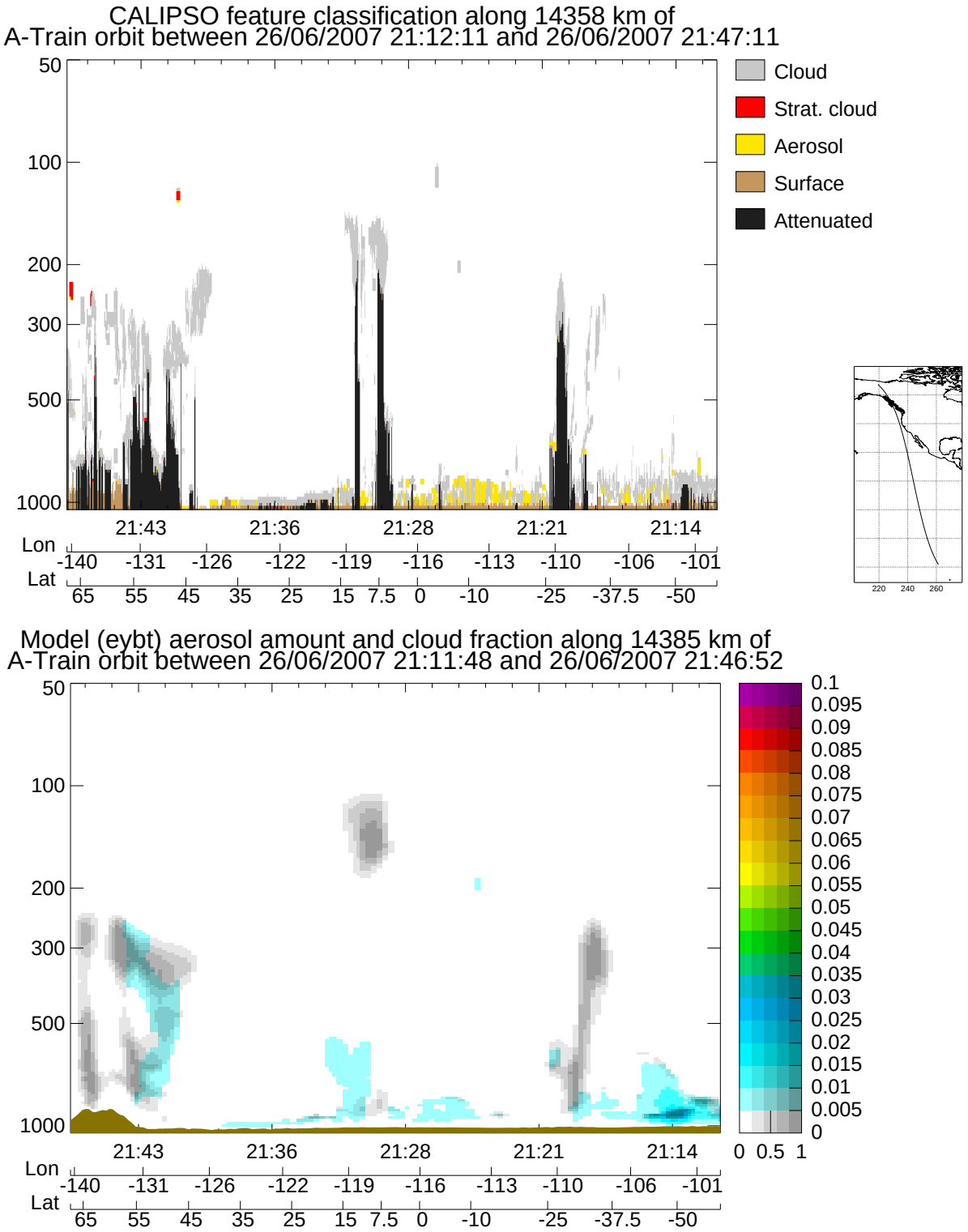

Figure 6.21: As in Figure 6.1, but for the orbit between 21:12:11 and 21:47:11.

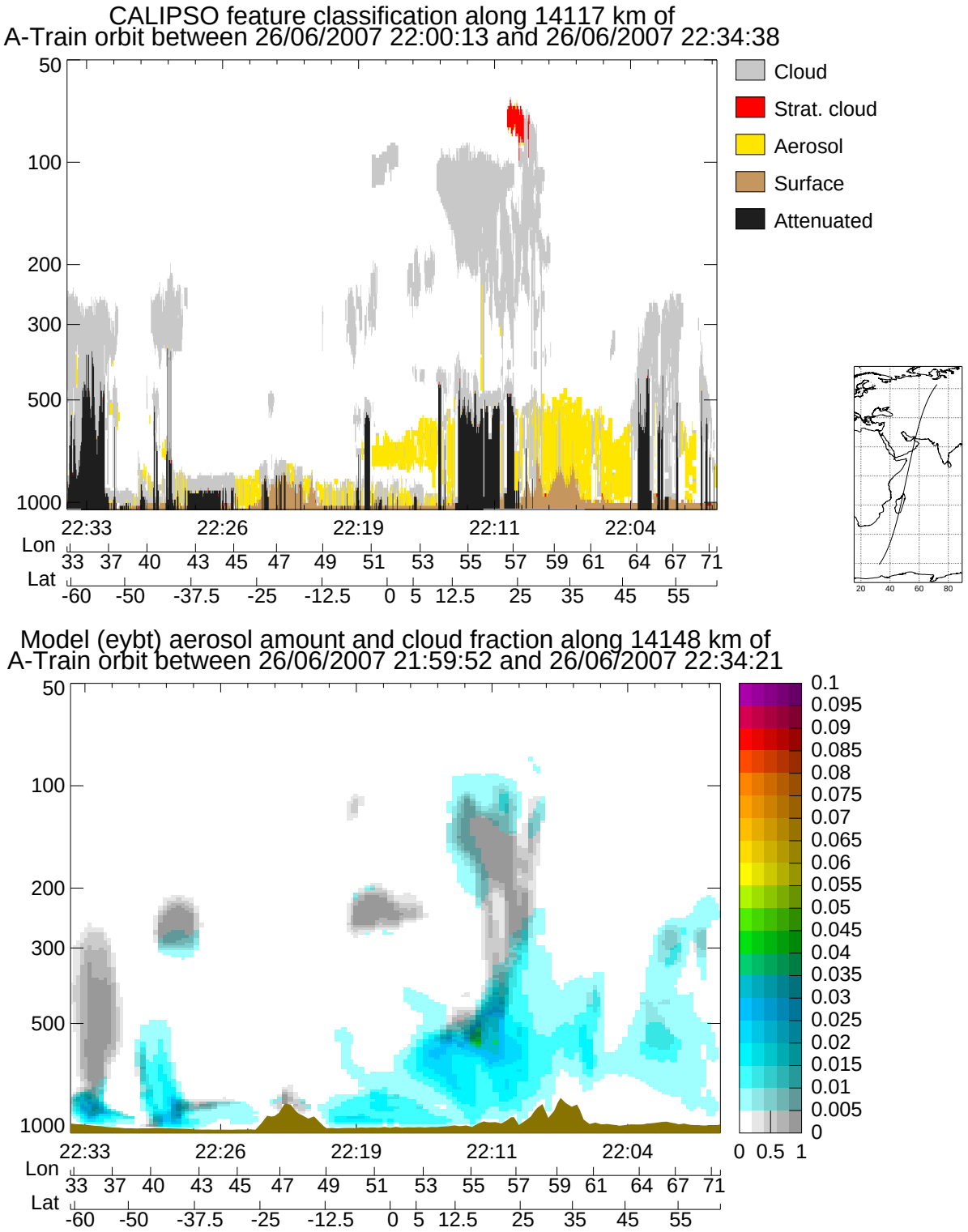

Figure 6.22: As in Figure 6.1, but for the orbit between 22:00:13 and 22:34:38.

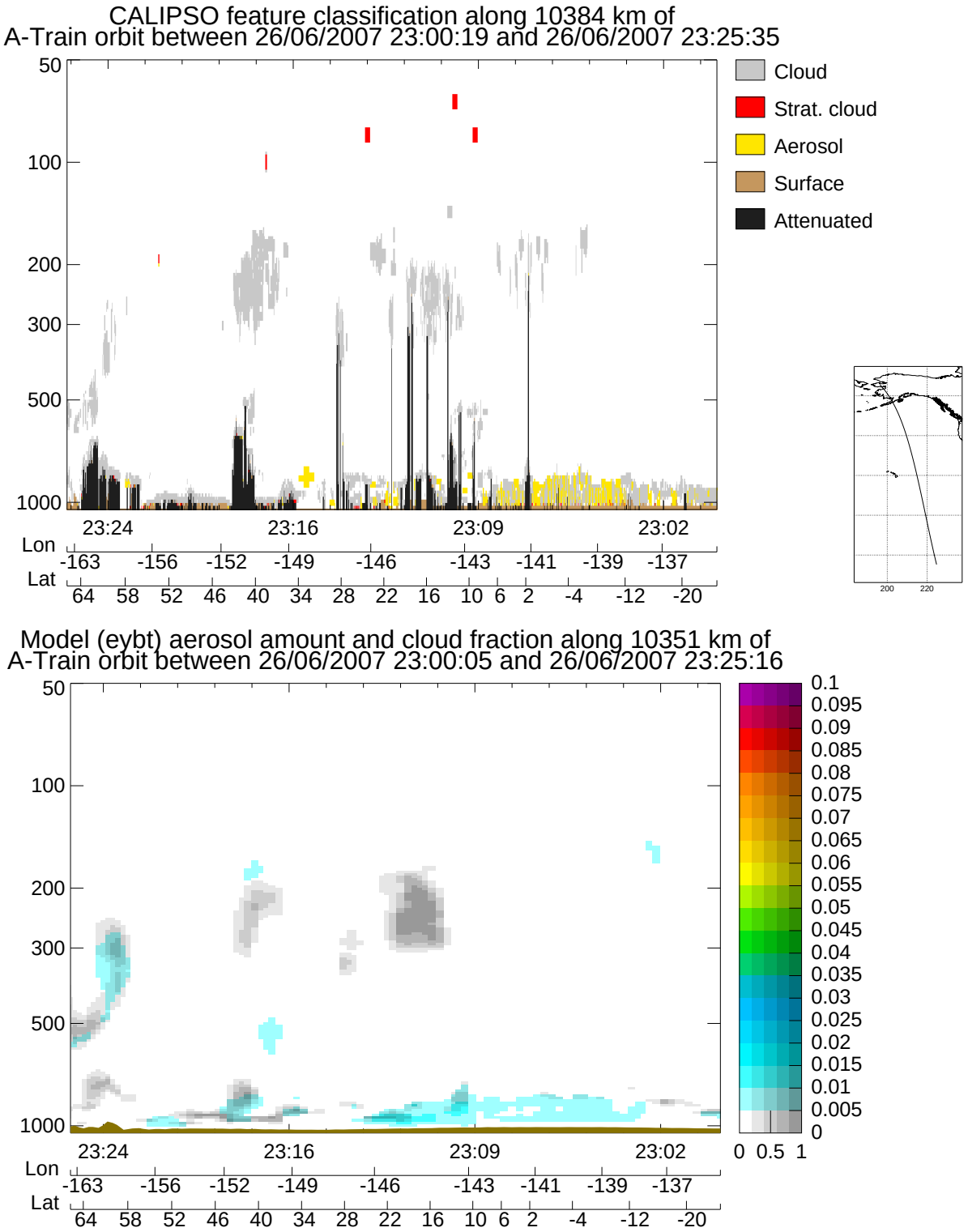

Figure 6.23: As in Figure 6.1, but for the orbit between 23:00:19 and 23:25:35.

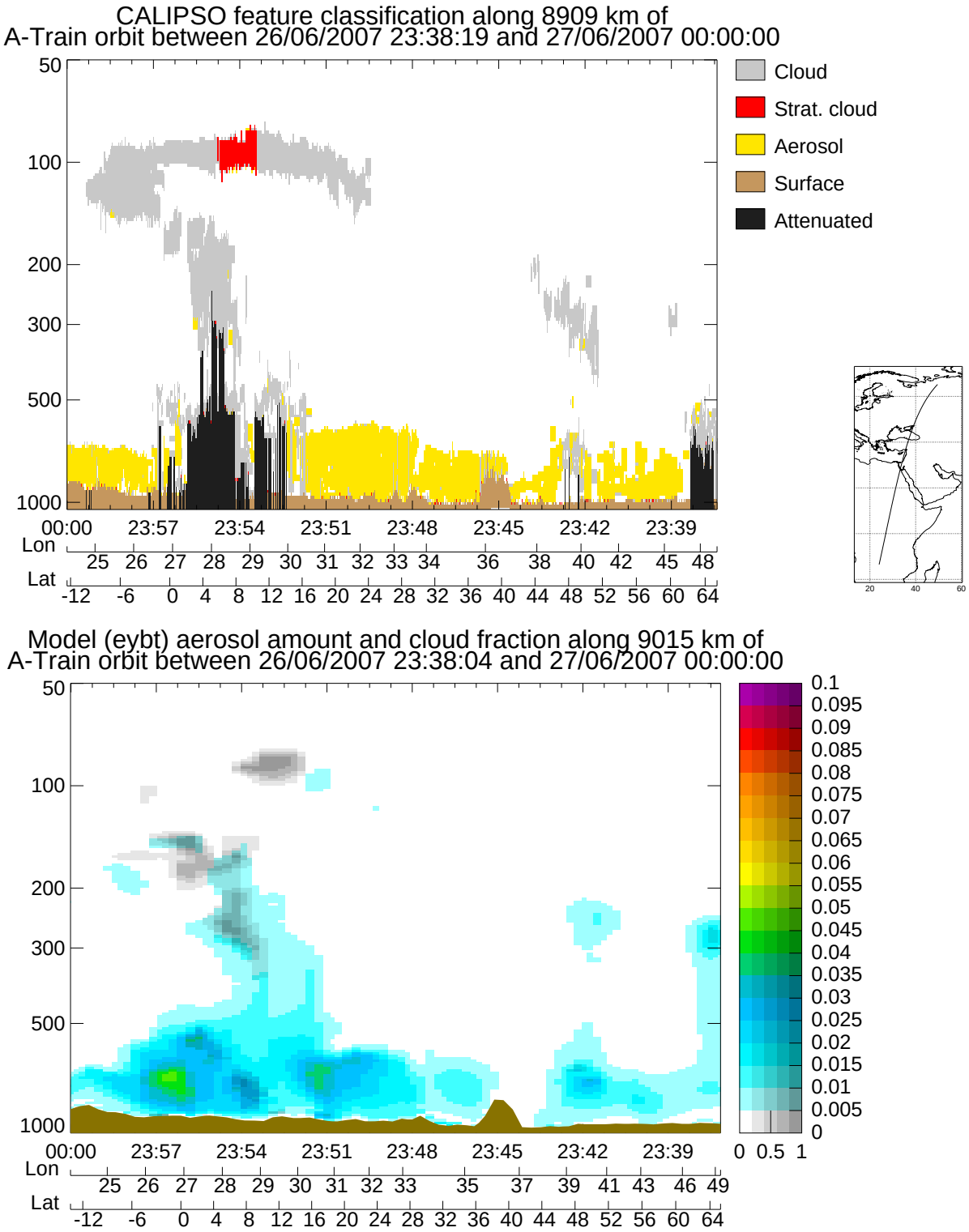

Figure 6.24: As in Figure 6.1, but for the orbit between 23:38:19 and 00:00:00.

7 Conclusion and perspectives

This study has focused on the vertical distribution of the aerosols in an experimental version of the ECMWF forecast system. The quality of this distribution has been assessed through comparisons with the cloud/aerosol mask derived from CloudSat/CALIPSO. Although such comparisons can appear limited in scope, it was felt that, before checking details, the large-scale features have to be shown to be realistic, and simple qualitative comparisons using the cloud/aerosol mask already brought potential problems into light. As such, this study has an exploratory character but still gives clear indications about the potential of space lidar observations. The comparisons were shown for one day randomly chosen, but should be representative of the behaviour of the model in normal circumstances. This study has concentrated solely on the forward model providing the trajectory calculations used for the 4D-Var assimilation of aerosol-related observations discussed in Benedetti *et al.* (2009).

The experimental aerosol model discussed here will undergo further developments. However, the results presented here show that this version of the IFS including a relatively simple prognostic representation of the main aerosols produces reasonable stand-alone forecasts even without a previous aerosol analysis. Therefore, it already offers a good starting point for the analysis of aerosol-related observations into the 4D-Var assimilation system. One of the priorities will be to decrease further the bias in the forward model. Again, it has to be stressed that the forward model discussed here might not include all the sophistication encountered in some climate-orientated general circulation models including prognostic aerosols. In the configuration described here, the forecast takes about twice as long as a forecast run without aerosols. The increased cost stems from the larger number of 3-D prognostic variables (from six used operationally to 18 in the model with prognostic aerosols) and a more involving package of physical parametrisations including those for aerosol-relevant processes. The model presented here offers a good trade-off between the computer efficiency and the quality of the resulting aerosol fields, both required for use as forward model in an analysis scheme.

How successful the model is at reproducing the temporal variability of the aerosol load depends mainly on the quality of the model dynamics. In that respect, results reported elsewhere (Morcrette *et al.*, 2009; Benedetti *et al.*, 2009) indicate that the model advection is very dependable in distributing the aerosols horizontally in overall agreement with satellite and surface observations of the aerosol optical depth.

The comparison with CALIPSO observations discussed in this part of the report addressed the vertical distribution through comparisons with CALIPSO observations. What appears as an erroneous vertical distribution of the model aerosols has been shown occurring usually for aerosols of anthropogenic origins (whether organic or black carbon or sulphate). This is often linked to a deficient information on the sources of these anthropogenic aerosols upstream of the observation area. A more important cause for concern is what appears to be a too strong transport by convection in the model, again mainly of the anthropogenic aerosols, but could simply reflect the limitations of the cloud/aerosol classification from CALIPSO observations. In this respect, two avenues of research are open, either sensitivity tests with the model including various changes to the inclusion of aerosol processes in presence of convection, or a possible refinement of the retrieval algorithms that would allow to obtain concurrent aerosol and cloud parameters in presence of convection. Such a possibility is clearly out of the scope of the present study, but should be considered when future radar/lidar algorithms are developed in the coming years.

The quality of the results of the forward model depends not only on the dynamics of the model and the adequacy of the aerosol physical parametrisations, but also on the representativeness of the sources. With the exact sources of aerosols (in particular, those of anthropogenic origin) not available in real time, the aerosol analysis, through the assimilation of aerosol-related observations, will provide initial conditions more representative of the true aerosol distribution in the atmosphere. The development of a successful

aerosol analysis is therefore fundamental to the quality of the subsequent aerosol forecast. Here the forecast model including prognostic aerosols was shown to provide a reasonable basis for this analysis. In the GEMS analysis (Benedetti *et al.*, 2009) and the current near-real time aerosol forecast performed since July 2008, the optical depth at 550 nm from MODIS is used to constrain the total optical depth at 550 nm provided by the aerosol model during the 12-hour trajectory calculation. Information on aerosol profile, such as produced by CALIPSO, has not yet been used in the assimilation. A cloud/aerosol mask as used in this study could bring an important constraint on the system.

A characterization of the dominant aerosol type present at a given level (often referred to as speciation parameter) is also an important information for modellers to check their simulated aerosols. However, such characterization of aerosol type as was done from SEVIRI, ATSR, MERIS data (Peubey *et al.*, 2009) still seems to be in its infancy and not very reliable to constrain a model. It is hoped that EarthCARE by combining lidar and radiometer measurements might improve on the possibility of a reliable aerosol speciation from space. The profile of a quantity directly linked to the aerosol type/content like that of the back-scattering coefficient is an observation of choice to constrain not only the aerosol vertical distribution, but also other more quantitative aerosol characteristics, once the basic question of the presence or not of the aerosol at a given height is known with a reasonable degree of certainty. Such a profile could be assimilated via a lidar simulator (as discussed by Huneeus and Boucher, 2007), once such a tool (including its adjoint) is available that would be efficient enough to be included in the analysis system.

In conclusion, the weather forecast community has now reached a point where, together with the aerosol modelling community, it can produce reasonably looking real-time meteorological forecasts including aerosols. These are operational at the U.S. Naval Research Laboratory, the NASA GMAO, pre-operational as part of the GEMS now MACC (Monitoring Atmospheric Composition and Climate) project at ECMWF and will be likely to be operational at the UK MetOffice by the end of MACC in 2012. A number of regional weather forecast models are presently building their capability to use aerosol initial conditions from the ”big” centres for their own aerosol forecasts. Given the time-line of the official EarthCARE project, a large number of such weather centres could benefit enormously from the provision of real-time aerosol retrieval products from the EarthCARE observations.

Acknowledgements

The NASA CloudSat Project is kindly acknowledged for providing the CloudSat data. The authors are also grateful to the Goddard Earth Sciences Data and Information Services Center (GES DISC) for providing MODIS data used within the GEMS/MACC aerosol analyses and forecasts. Prof. G.L. Stephens, Drs M.J. Miller, A. Beljaars, M. Janisková and A. Benedetti are thanked for their comments on the paper.

A List of Acronyms

1D-/4D-Var	One-/Four-Dimensional Variational assimilation
AATSR	Advanced Along-Track Scanning Radiometer
AEROCOM	Aerosol Comparisons between Observations and Model
AERONET	Aerosol Robotic Network
BC	Black Carbon
CALIPSO	Cloud-Aerosol Lidar and Infrared Pathfinder Satellite Observation
CloudSat	NASA's cloud radar mission
DMS	dimethyl sulphide
DU	dust
EarthCARE	Earth, Clouds, Aerosols and Radiation Explorer
ECHAM-HAM	European Centre Hamburg Model - aerosol climate model
ECMWF	European Centre for Medium Range Weather Forecasts
EDGAR	Emission Database for Global Atmospheric Research
ESA	European Space Agency
GCM	General (or Global) Circulation Model
GEMS	Global and regional Earth-system (Atmosphere) Monitoring using Satellite and in-situ data
GES DISC	Goddard Earth Sciences Data and Information Services Center
GFED	Global Fire Emission Database
GMAO	Goddard Global Modeling and Assimilation Office
GOCART	Goddard Chemistry Aerosol Radiation and Transport
IFS	Integrated Forecasting System
INDOEX	Indian Ocean Experiment
LMD-Z	Laboratoire de Meteorologie Dynamique
LOA	Laboratoire d'Optique Atmospherique
MACC	Monitoring Atmospheric Composition and Climate
MERIS	Medium Resolution Imaging Spectrometer Instrument
MISR	Multi-angle Imaging SpectroRadiometer
MODIS	Moderate Resolution Imaging Spectroradiometer
NASA	National Aeronautics and Space Administration
OM	Organic Matter
SDS-WAS	Sand and Dust Storm Warning and Assessment System
SEVIRI	Spinning Enhanced Visible and Infra-Red Imager
SPEW	Speciated Particulate Emission Wizard
SS	Sea Salt
UTC	Coordinated Universal Time
UV	Ultraviolet
WMO	World Meteorological Organization

References

Benedetti, A., J.-J. Morcrette, O. Boucher, A. Dethof, R. J. Engelen, M. Fisher, H. Flentje, N. Huneeus, L. Jones, J. W. Kaiser, *et al.*, 2009: Aerosol analysis and forecast in the European Centre for Medium-Range Weather Forecasts Integrated Forecast System: 2. Data assimilation, *J. Geophys. Res.-Atmospheres*, **114**(D13), D13205, doi:10.1020/2008JD011115.

Boucher, O., M. Pham, and C. Venkataraman, 2002: Simulation of the atmospheric sulfur cycle in the LMD GCM. Model description, model evaluation, and global and European budgets, in *IPSL, Note 23, 26 pp. (available at http://www.ipsl.jussieu.fr/ poles/ Modelisation/ NotesSciences.htm.)*.

Chin, M., P. Ginoux, S. Kinne, O. Torres, B. N. Holben, B. N. Duncan, R. V. Martin, J. A. Logan, A. Higurashi, and T. Nakajima, 2002: Tropospheric aerosol optical thickness from the GOCART model and comparisons with satellite and Sun photometer measurements, *J. Atmos. Sci.*, **59**, 461–483.

Chin, M., D. J. Jacob, G. M. Gardner, and P. A. Spiro, 1996: A global three-dimensional model of tropospheric sulfate, *J. Geophys. Res.*, **101**, 18667–18690.

Clarke, A. D., W. G. Collins, P. J. Rasch, V. N. Kapustin, K. Moore, S. Howell, and H. E. Fuelber, 2001: Dust and pollution transport on global scales: Aerosol measurements and model predictions, *J. Geophys. Res.*, **106D**, 32555–32570, doi: 10.1029 /2000JD900842.

Collins, W. D., P. J. Rasch, B. E. Eaton, B. V. Khattatov, J.-F. Lamarque, and C. S. Zender, 2001: Simulating aerosols using a chemical transport model with assimilation of satellite aerosol retrievals: Methodology for INDOEX, *J. Geophys. Res.*, **106D**, 7313–7336, doi: 10.1029 /2000JD900507.

Croft, B., U. Lohmann, R. V. Martin, P. Stier, S. Wurzler, J. Feichter, C. Hoose, U. Heikkilä, A. van Donkelaar, and S. Ferrachat, 2009a: Influences of in-cloud aerosol scavenging parameterizations on aerosol concentrations and wet deposition in ECHAM5-HAM, *Atmos. Chem. Phys. Discucc.*, **9**, 22041–22101.

Croft, B., U. Lohmann, R. V. Martin, P. Stier, S. Wurzler, J. Feichter, R. Posselt, and S. Ferrachat, 2009b: Aerosol size-dependent below-cloud scavenging by rain and snow in the ECHAM5-HAM, *Atmos. Chem. Phys.*, **9**, 4653–4675.

Dentener, F., J. Feichter, and A. Jeuken, 1999: Simulation of the transport of 222Rn using on-line and off-line models at different horizontal resolutions: A detailed comparison with observations, *Tellus*, **51B**, 573–602.

Dentener, F., S. Kinne, T. Bond, O. Boucher, J. Cofala, S. Generoso, P. Ginoux, S. Gong, J. J. Hoelzemann, A. Ito, L. Marelli, J. E. Penner, J.-P. Putaud, C. Textor, M. Schulz, G. R. van der Werf, and J. Wilson, 2006: Emissions of primary aerosol and precursor gases in the years 2000 and 1750 prescribed data-sets for AeroCom, *Atmos. Chem. Phys.*, **6**, 4321–4344.

Dubovik, O., B. Holben, T. F. Eck, A. Smirnov, Y. J. Kaufman, M. King, D. Tanré, and I. Slutsker, 2002: Variability of absorption and optical properties of key aerosol types observed in worldwide locations, *J. Atmos. Sci.*, **59**, 590–608.

Feichter, J. and U. Lohmann, 1999: Can relaxation technique be used to validate clouds and sulphur species in a GCM?, *Quart. J. Roy. Meteor. Soc.*, **125**, 1277–1294.

Genthon, C., 1992: Simulations of desert dust and sea salt aerosols in Antarctica with a general circulation model of the atmosphere, *Tellus*, **44B**, 371–389.

Gillette, D., J. Adams, A. Endo, and D. Smith, 1980: Threshold velocities for input of soil particles in the air by desert soils, *J. Geophys. Res.*, **85**, 5621–5630.

Ginoux, P., M. Chin, I. Tegen, J. M. Prospero, B. Holben, O. O. Dubovik, and S.-J. Lin, 2001: Sources and distributions of dust aerosols simulated with the GOCART model, *J. Geophys. Res.*, **106D**, 20255–20274.

Giorgi, F., 1986a: A particle dry deposition parameterization scheme for use in tracer transport models, *J. Geophys. Res.*, **91D**, 9794–9806.

Giorgi, F., 1986b: Development of an Atmospheric Aerosol Model for Studies of Global Budgets and Effects of Airborne Particulate Material, in *Ph. D. thesis, Georgia Instit. Technol., Atlanta, Georgia, USA*.

Giorgi, F. and W. L. Chameides, 1986: Rainout lifetimes of highly soluble aerosols and gases as inferred from simulations with a general circulation model, *J. Geophys. Res.*, **91D**, 14367–14376.

Gong, S. L., L. A. Barrie, and J.-P. Blanchet, 1997: Modeling sea-salt aerosols in the atmosphere. 1. Model development, *J. Geophys. Res.*, **102D**, 3805–3818.

Gong, S. L., L. A. Barrie, J.-P. Blanchet, K. V. Salzen, U. Lohmann, G. Lesins, L. Spacek, L. M. Zhang, E. Girard, H. Lin, R. Leaitch, H. Leighton, P. Chylek, and P. Huang, 2003: Canadian Aerosol Module: A Size Segregated Simulation of Atmospheric Aerosol Processes for Climate and Air Quality Models 1. Module Development, *J. Geophys. Res.*, **108(D1)**, 4007, doi: 10.1029 /2001JD002002.

Grini, A., G. Myrhe, J. K. Sundet, and I. S. A. Isaksen, 2002: Modeling the annual cycle of sea salt in the global 3D model Oslo CTM2: Concentrations, fluxes and radiative impact, *J. Climate*, **15**, 1717–1730.

Guelle, W., Y. J. Balkanski, M. Schulz, F. Dulac, and P. Monfray, 1998: Wet deposition in a global size-dependent aerosol transport model. 1. Comparison of a 1 year 210Pb simulation with ground measurements, *J. Geophys. Res.*, **103D**, 11429–11445.

Guelle, W., Y. J. Balkanski, M. Schulz, B. Marticorena, G. Bergametti, C. Moulin, R. Arimoto, and K. D. Perry, 2000: Modeling the atmospheric distribution of mineral aerosol: Comparison with ground and satellite observations for yearly and synoptic timescales over the North Atlantic, *J. Geophys. Res.*, **105D**, 1997–2012.

Guelle, W., M. Schulz, Y. J. Balkanski, and F. Dentener, 2001: Influence of the source formulation on modeling the atmospheric global distribution of sea salt, *J. Geophys. Res.*, **106D**, 27509–27524.

Holben, B. N., T. F. Eck, I. Slutsker, D. Tanré, J. P. Buis, A. Setzer, E. Vermote, J. A. Reagan, Y. J. Kaufman, T. Nakajima, F. Lavenu, I. Jankowiak, and A. Smirnov, 1998: An emerging ground-based aerosol climatology: Aerosol optical depth from AERONET, *J. Geophys. Res.*, **103D**, 12067–12097.

Hollingsworth, A., R. J. Engelen, C. Textor, A. Benedetti, O. Boucher, F. Chevallier, A. Dethof, H. Elbern, H. Eskes, J. Flemming, C. Granier, J. W. Kaiser, J.-J. Morcrette, P. Rayner, V.-H. Peuch, L. Rouil, M. Schultz, A. Simmons, and the GEMS Consortium, 2008: The Global Earth-system Monitoring using Satellite and in-situ data (GEMS) project: Towards a monitoring and forecasting system for atmospheric composition., *Bull. Amer. Meteor. Soc.*, **89**, 1147–1164, doi: 10.1175 /2008BAMS2355.1.

Huneeus, N. and O. Boucher, 2007: One-dimensional variational retrieval of aerosol extinction coefficient from synthetic LIDAR and radiometric measurements, *J. Geophys. Res.*, **112**(D14), D14303, doi:10.1029/2006/JD007625.

Jeuken, A. B. M., P. C. Siegmund, L. C. Heijboer, J. Feichter, and L. Bengtsson, 1996: On the potential of assimilating meteorological analyses in a global climate model for the purpose of model validation, *J. Geophys. Res.*, **101**, 16939–16950.

Joussaume, S., 1990: Three-dimensional simulations of the atmospheric cycle of desert dust particles using a general circulation model, *J. Geophys. Res.*, **95D**, 1909–1941.

Kinne, S., U. Lohmann, J. Feichter, M. Schulz, C. Timmreck, S. Ghan, R. Easter, M. Chin, P. Ginoux, T. Takemura, I. Tegen, D. Koch, M. Herzog, J. Penner, P. G., B. Holben, T. Eck, A. Smirnow, O. Dubovik, I. Slutsker, D. Tanré, O. Torres, M. Mishchenko, I. Geogdzhayev, D. A. Chu, and Y. Kaufman, 2003: Monthly averages of aerosol properties: A global comparison among models, satellite data, and AERONET ground data, *J. Geophys. Res.*, **108, (D20)**, 4634, doi:10.1029/2001JD001253.

Kinne, S., M. Schulz, C. Textor, S. Guibert, Y. Balkanski, S. E. Bauer, T. Berntsen, T. F. Berglen, O. Boucher, M. Chin, W. Collins, F. Dentener, T. Diehl, R. Easter, J. Feichter, D. Fillmore, S. Ghan, P. Ginoux, S. Gong, A. Grini, J. Hendricks, M. Herzog, L. Horowitz, I. Isaksen, T. Iversen, A. Kirkevåg, S. Kloster, D. Koch, J. E. Kristjansson, M. Krol, A. Lauer, J. F. Lamarque, G. Lesins, X. Liu, U. Lohmann, V. Montanaro, G. Myhre, J. Penner, G. Pitari, S. Reddy, O. Seland, P. Stier, T. Takemura, and X. Tie, 2006: An AeroCom initial assessment: Optical properties in aerosol component modules of global models, *Atmos. Chem. Phys.*, **6**, 1815–1834.

Laurent, B., B. Heinold, I. Tegen, C. Bouet, and G. Cautenet, 2008: Surface wind accuracy for modeling mineral dust emissions: Comparing two regional models in a Bodélé case study, *Geophys. Res. Letters*, **35**, L09804, doi: 10.1029 /2008GL033654.

Lee, H. N. and H. Feichter, 1995: An intercomparison of wet precipitation scavenging schemes and the emission rates of ^{222}Rn for the simulation of global transport and deposition of ^{210}Pb, *J. Geophys. Res.*, **100D**, 23253–23270.

Liousse, C., J. E. Penner, C. Chuang, J. J. Walton, H. Eddleman, and H. Cachier, 1996: A global three-dimensional model study of carbonaceous aerosols, *J. Geophys. Res.*, **101**, 19411–19432.

Liu, M., D. L. Westphal, S. Wang, A. Shimizu, N. Sugimoto, J. Zhou, and Y. Chen, 2003: A high-resolution numerical study of the Asian dust storms of April 2001, *J. Geophys. Res.*, **108D**, 8653, doi: 10.1029 /2002JD003178.

Marticorena, B. and G. Bergametti, 1995: Modelling the atmospheric dust cycle. 1: Design of a soil-derived dust emission scheme, *J. Geophys. Res.*, **100**, 16415–16430.

Massey, M. R., 1987: The gravitational settling of aerosol particles in homogeneous turbulence and random flow fields, *J. Fluid Mech.*, **174**, 441–465.

Monahan, E. C., K. L. Davidson, and D. E. Spiel, 1986: Whitecap aerosol productivity deduced from simulation tank measurements, *J. Geophys. Res.*, **87**, 8898–8904.

Morcrette, J.-J., A. Beljaars, A. Benedetti, L. Jones, and O. Boucher, 2008: Sea-salt and dust aerosols in the ECMWF IFS, *Geophys. Res. Lett.*, **35**, L24813, doi: 10.1029 /2008GL036041.

Morcrette, J.-J., O. Boucher, L. Jones, D. Salmond, P. Bechtold, A. Beljaars, A. Benedetti, A. Bonet, J. W. Kaiser, M. Razinger, *et al.*, 2009: Aerosol analysis and forecast in the European Centre for Medium-Range Weather Forecasts Integrated Forecast System: Forward modeling, *J. Geophys. Res.-Atmospheres*, **114**(D6), D06206, doi: 10.1029 /2008JD011235.

O'Dowd, C. D., M. H. Smith, I. E. Consterdine, and J. A. Lowe, 1997: Marine aerosol, sea salt, the marine sulphur cycle: A short review, *Atmos. Environ.*, **31**, 73–80.

Penner, J. E., S. Y. Zhang, M. Chin, C. C. Chuang, J. J. Feichter, Y. Feng, I. V. Geogdzhayev, P. Ginoux, M. M. Herzog, A. Higurashi, D. Koch, C. Land, U. Lohmann, M. Mishchenko, T. Nakajima, G. Pitari, B. Soden, I. Tegen, and L. Stowe, 2002: A comparison of model- and satellite-derived aerosol optical depth and reflectivity, *J. Atmos. Sci.*, **59**, 441–460.

Peubey, C., A. Benedetti, L. Jones, and J.-J. Morcrette, 2009: GEMS-AAerosol: Comparison and analysis with GlobAEROSOL data, in *GlobAEROSOL User Report, October 2009*, pp. 11–20.

Rasch, P. J., W. D. Collins, and B. E. Eaton, 2001: Understanding the Indian Ocean Experiment (INDOEX) aerosol distributions with an aerosol assimilation, *J. Geophys. Res.*, **106(D7)**, 7337–7356.

Rasch, P. J., J. Feichter, K. Law, N. Mahowald, J. Penner, and et al, 2000: An assessment of scavenging and deposition processes in global models: Results from the WCRP Cambridge workshop of 1995, *Tellus*, **52B**, 1025–1056.

Reddy, M. S., O. Boucher, N. Bellouin, M. Schulz, Y. Balkanski, J.-L. Dufresne, and M. Pham, 2005: Estimates of global multicomponent aerosol optical depth and direct radiative perturbation in the Laboratoire de Meteorologie Dynamique general circulation model, *J. Geophys. Res.*, **110D**, S16, doi: 10.1029 /2004JD004757.

Reddy, M. S., O. Boucher, C. Venkataraman, S. Verma, J.-F. Léon, N. Bellouin, and M. Pham, 2004: General circulation model estimates of aerosol transport and radiative forcing during the Indian Ocean Experiment, *J. Geophys. Res.*, **109**, D16205, doi: 10.1029/2004JD004557.

Remer, L. A., Y. J. Kaufman, D. Tanré, S. Mattoo, D. A. Chu, J. V. Martins, R.-R. Li, C. Ichoku, R. C. Levy, R. G. Kleidman, T. F. Eck, E. Vermotte, and B. N. Holben, 2005: The MODIS aerosol algorithm, products and validation, *J. Atmos. Sci.*, **62**, 947–973.

Schulz, M., G. de Leeuw, and Y. J. Balkanski, 2004: Sea-salt aerosol source functions and emissions, in *Emission of Atmospheric Trace Compounds, ed. by C. Granier, P. Artaxo, and C.E. Reeves, Kluwer Acad. Norwell, Mass*, pp. 333–354.

Schulz, M., C. Textor, S. Kinne, Y. Balkanski, S. Bauer, T. Berntsen, T. Berglen, O. Boucher, F. Dentener, S. Guibert, I. S. A. Isaksen, T. Iversen, D. Koch, A. Kirkevåg, X. Liu, V. Montanaro, G. Myhre, J. E. Penner, G. Pitari, S. Reddy, O. Seland, P. Stier, and T. Takemura, 2006: Radiative forcing by aerosols as derived from the AeroCom present-day and pre-industrial simulations, *Atmos. Chem. Phys.*, **6**, 5225–5246.

Sekiyama, T. T., T. Y. Tanaka, A. Shimizu, and T. Miyoshi, 2009: Data assimilation of CALIPSO aerosol observations, *Atmos. Chem. Phys. Discuss.*, **9**, 5785–5808.

Shao, Y., Y. Yang, J. Wang, Z. Song, L. M. Leslie, C. Dong, Z. Zhang, Z. Lin, Y. Kanai, S. Yabuki, and Y. Chun, 2003: Northeast Asian dust storms: Real-time numerical prediction and validation, *J. Geophys. Res.*, **108**, 4691, doi: 10.1029 /2003JD003667.

Slinn, S. A. and W. G. N. Slinn, 1980: Predictions for particle deposition on natural waters, *Atmos. Environ.*, **14**, 1013–1016.

Slinn, W. G. N., 1982: Predictions for particle deposition to vegetative canopies, *Atmos. Environ.*, **16**, 1785–1794.

Smith, M. H. and N. M. Harrison, 1998: The sea spray generation function, *J. Aersol Sci.*, **29**, Suppl.1, S189–S190.

Smith, M. H., P. M. Park, and I. E. Consterdine, 1993: Marine aerosol concentrations and estimated fluxes over the sea, *Quart. J. Roy. Meteor. Soc.*, **119**, 809–824.

Stephens, G. L., D. G. Vane, R. J. Boain, G. G. Mace, K. Sassen, Z. Wang, A. J. Illingworth, E. J. O'Connor, W. B. Rossow, S. L. Durden, *et al.*, 2002: The Cloudsat mission and the A-Train, *Bull. Amer. Meteor. Soc.*, **83**, 1771–1790.

Tegen, I. and I. Fung, 1994: Modeling of mineral dust in the atmosphere: Sources , transport, and optical thickness, *J. Geophys. Res.*, **99**, 22897–22914.

Tegen, I., P. Hoorig, M. Chin, I. Fung, D. Jacob, and J. Penner, 1997: Contribution of different aerosol species to the global aerosol extinction optical thickness: Estimates from model results, *J. Geophys. Res.*, **102**, 23895–23915.

Textor, C., M. Schulz, S. Guibert, S. Kinne, Y. Balkanski, S. Bauer, T. Berntsen, T. Berglen, O. Boucher, M. Chin, F. Dentener, T. Diehl, R. Easter, H. Feichter, D. Fillmore, S. Ghan, P. Ginoux, S. Gong, A. Grini, J. Hendricks, L. Horowitz, P. Huang, I. Isaksen, I. Iversen, S. Kloster, D. Koch, A. Kirkevåg, J. E. Kristjansson, M. Krol, A. Lauer, J. F. Lamarque, X. Liu, V. Montanaro, G. Myhre, J. Penner, G. Pitari, S. Reddy, O. Seland, P. Stier, T. Takemura, and X. Tie, 2006: Analysis and quantification of the diversities of aerosol life cycles within AeroCom, *Atmos. Chem. Phys.*, **6**, 1777–1813.

Textor, C., M. Schulz, S. Guibert, S. Kinne, Y. Balkanski, S. Bauer, T. Berntsen, T. Berglen, O. Boucher, M. Chin, F. Dentener, T. Diehl, J. Feichter, D. Fillmore, P. Ginoux, S. Gong, A. Grini, J. Hendricks, L. Horowitz, P. Huang, I. S. A. Isaksen, T. Iversen, S. Kloster, D. Koch, A. Kirkevåg, J. E. Kristjansson, M. Krol, A. Lauer, J. F. Lamarque, X. Liu, V. Montanaro, G. Myhre, J. E. Penner, G. Pitari, M. S. Reddy, O. Seland, P. Stier, T. Takemura, and X. Tie, 2007: The effect of harmonized emissions on aerosol properties in global models: an AeroCom experiment, *Atmos. Chem. Phys.*, **7**, 4489–4501.

Tompkins, A. M., 2005: A revised cloud scheme to reduce the sensitivity to vertical resolution, *ECMWF Research Dept Technical Memorandum*, p. 20 pp.

Uno, I., Z. Wang, M. Chiba, Y. S. Chun, S. L. Gong, Y. Hara, E. Jung, S.-S. Lee, M. Liu, M. Mikami, S. Music, S. Nickovic, S. Satake, Y. Shao, Z. Song, N. Sugimoto, T. Tanaka, and D. L. Westphal, 2006: Dust model intercomparison (DMIP) study over Asia: Overview, *J. Geophys. Res.*, **111**, D12213, doi: 10.1029 /2005JD006575.

Vaughan, M. A., D. M. Winker, and K. A. Powell, 2005: *CALIOP Algorithm Theoretical Basis Document. Part 2: Feature detection and layer properties algorithms. PC-SCI-202 Part 2, Release 1.01, 27 September 2005*.

Vignati, E., J. Wilson, and P. Stier, 2004: An efficient size-resolved aerosol microphysics module for large-scale aerosol transport models, *J. Geophys. Res.*, **109**, D22202, doi: 10.1029 /2003JD004485.

Wisely, M. L. and B. B. Hicks, 2000: A review of the current status of knowledge on dry deposition, *Atmos. Environ.*, **34**, 2261–2282.

Witek, M. L., P. J. Flatau, P. K. Quinn, and D. L. Westphal, 2007a: Global sea-salt modeling: Results and validation against multi-campaign shipboard measurements., *J. Geophys. Res.*, **112**, D08215, doi:10.1029/2006JD007779.

Witek, M. L., P. J. Flatau, J. Teixeira, and D. L. Westphal, 2007b: Coupling an ocean wave model with a global aerosol transport model: A sea salt aerosol parameterization perspective, *Geophys. Res. Lett.*, **34**, L14806, doi:10.1029/2007GL030106.

Zhang, J. and J. S. Reid, 2006: MODIS Aerosol Product Analysis for Data Assimilation: Assessment of Level 2 Aerosol Optical Thickness Retrievals, *J. Geophys. Res*, **111**, D22207, doi:10.1029/2005JD006898.

Zhang, J., J. S. Reid, and B. N. Holben, 2005: An analysis of potential cloud artifacts in MODIS over ocean aerosol optical thickness products, *Geophys. Res. Lett.*, **32**, L15803, doi:10.1029/2005GL023254.

Zhang, J., J. S. Reid, D. Westphal, N. Baker, and E. Hyer, 2008: A System for Operational Aerosol Optical Depth Data Assimilation over Global Oceans, *J. Geophys. Res*, **113**, D10208, doi:10.1029/2007JD009065.

Zhao, T. L., S. L. Gong, X. Y. Zhang, A. Abdel-Mawgoud, and Y. P. Shao, 2006: An assessment of dust emission schemes in modeling East Asian dust storms, *J. Geophys. Res.*, **111**, D05590, doi: 10.1029 /2004JD005746.

Zhao, T. L., S. L. Gong, X. Y. Zhang, and I. G. Mckendry, 2003: Modeled size segregated wet and dry deposition budgets of soil dust aerosol during ACE-Asia 2001: Implications for trans-Pacific transport, *J. Geophys. Res.*, **108**, 8665, doi: 10.1029/2002JD003363.

Zhou, C. H., S. L. Gong, X. Y. Zhang, Y. Q. Wang, T. Niu, H. L. Liu, T. L. Zhao, Y. Q. Yang, and Q. Hou, 2008: Development and evaluation of an operational SDS forecasting system for East Asia: CUACE/Dust, *Atmos. Chem. Phys.*, **8**, 787–798.